Journal of Medicinal Chemistry

Volume 50, Number 3 February 8, 2007

Perspective

Molecular Recognition of Protein Kinase Binding Pockets for Design of Potent and Selective Kinase Inhibitors

Jeffrey Jie-Lou Liao*

TransTech Pharma, 4170 Mendenhall Oaks Parkway, High Point, North Carolina 27265, and Department of Chemistry, Duke University, Durham, North Carolina 27708

Received July 10, 2006

Introduction

Protein kinases constitute one of the largest protein families in humans.[1,2] The kinase enzymes in this family catalyze phosphorylation of serine, threonine, or tyrosine residues, regulate the majority of signal transduction pathways in cells, and thus play an important role in cell growth, metabolism, differentiation, and apoptosis. Deregulation of protein kinases is implicated in a number of diseases including cancer, diabetes, and inflammation. Targeted inhibition of protein kinases has thereby become an attractive therapeutic strategy in the treatment of relevant diseases.[3−7]

All kinase enzymes share a catalytic domain that contains a cleft where adenosine triphosphate (ATP[a]) binds. This catalytic cleft is a major focus of small-molecule drug design for protein kinases. Breakthrough advances over the past decade have so far resulted in several small-molecule kinase inhibitors approved for clinical use by U.S. Food and Drug Administration (FDA). These kinase drugs include imatinib mesylate (STI571, **1**)[8,9] (Novartis, 2001), gefitinib (ZD1839, **2**)[10] (AstraZeneca, 2003), erlotinib (OSI 774, **3**)[11] (Genentech and OSIP, 2004), sorafenib tosylate (Bay 43-9006, **4**)[12] (Bayer and Onyx, 2005), sunitinib malate (SU11248, **5**)[13] (Pfizer, 2006), and dasatinib (BMS-354825, **6**)[14] (Bristol-Myers Squibb, 2006). Their structural formulas are given in Figure 1. The successes of these drugs in specific patient populations have stimulated enthusiasm for investment in the field. Currently, it is estimated that approximately one-third of drug discovery programs target protein kinases.[5] Despite the substantial achievements in protein kinase drug discovery, design of potent inhibitors with high degrees of selectivity during lead optimization remains a major challenge. Many kinase inhibitors have failed in preclinical or clinical development because of the lack of such selectivity that induces intolerable side effects, mostly because the catalytic cleft is highly conserved in sequence and conformation.[4,5,15−18] Systematic analysis of the crystal structures of protein kinases can offer insight into the design of highly selective kinase inhibitors to overcome these effects.

Some 50 unique crystal structures of protein kinase catalytic domains have been published in the Protein Data Bank[19−22] since the first X-ray structure of a kinase domain was determined for cAMP-dependent kinase (PKA) in 1991.[23] To address the issue of how to design highly potent and selective kinase inhibitors, this review provides detailed structural analysis, focusing on important protein kinase targets and their relevant reversible small-molecule inhibitors (Figure 1) with available and updated structural information. This article first analyzes the catalytic cleft and its binding pockets in active and inactive states. The

* Correspondence address: TransTech Pharma, 4170 Mendenhall Oaks Parkway, High Point, NC 27708. Phone: 336-841-0300, extension 129. Fax: 336-841-0310. E-mail: jliao@ttpharma.com.

[a] Abbreviations: ATP, adenosine triphosphate; FDA, Food and Drug Administration; PKA, cAMP-dependent kinase; N-lobe, N-terminal lobe; C-lobe, C-terminal lobe; CDK2, cyclin-dependent kinase 2; PDB, Brookhaven Protein Data Bank; αC, αC helix; G-loop, glycine-rich loop; A-segment, activation segment; A-loop, activation loop; EGFR, epidermal growth factor receptor tyrosine kinase; c-Kit, stem cell factor receptor tyrosine kinase; c-Abl, Abelson leukemia virus tyrosine kinase; MAP, mitogen-activated protein kinase; AGC, protein kinases A, G, and C subfamilies; PKB, protein kinase B; ROCK, Rho-associated coiled−coiled containing protein kinase; BP, binding pocket; GTP, guanine triphosphate; CK2, casein kinase II; IRK, insulin receptor tyrosine kinase; VEGFR, vascular endothelial growth factor receptor tyrosine kinase; Flt3, Fms-like tyrosine kinase 3; SH, Src homology domain; FGFR, fibroblast growth factor receptor tyrosine kinase; GIST, gastrointestinal stromal tumor; MEK, MAP kinase kinase; ERK, extracellular signal-regulated kinase; PDGFR, platelet derived growth factor receptor tyrosine kinase; CML, chronic myelogenous leukemia; GSK, glycogen synthase kinase; NSCLC, non-small-cell lung cancer; PK, pharmacokinetic; PD, pharmacodynamic.

10.1021/jm0608107 CCC: $37.00
Published on Web 01/10/2007

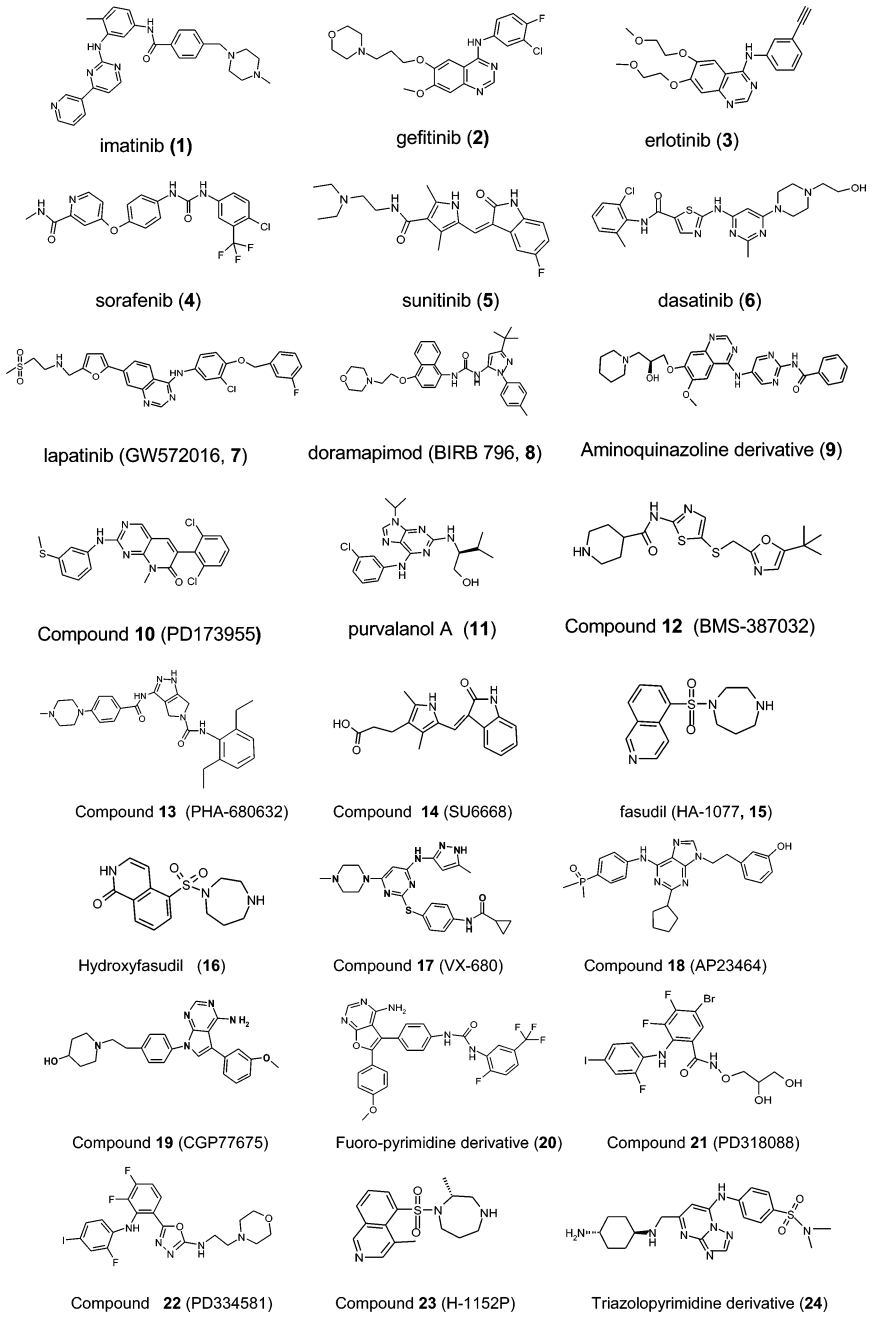

Figure 1. Structural formulas of compounds **1**−**24**.

modes in which high-affinity inhibitors bind to different combinations of the pockets are systematically classified and illustrated in Figures 14−20. Specificity determinants for the binding pockets and molecular recognition of these specificities critical for design of highly selective inhibitors are presented.

Binding Pockets in the Kinase Catalytic Cleft

The Catalytic Cleft. The catalytic domain of a protein kinase comprises two lobes, an N-terminal lobe (N-lobe) and a larger C-terminal lobe (C-lobe). The catalytic cleft is formed between these two lobes. Here, the crystal structure of active cyclin-dependent kinase 2 (CDK2) (PDB code 1QMZ)[24] is used. As shown in Figure 2, the N-lobe consists of β strands predominantly, which form the ceiling of the cleft, and one α helix (αC). The C-lobe is mainly α -helical. The two lobes are connected with a linker including a hinge and a convex-shaped motif (E_0 in Figure 2). The N-lobe contains a consensus glycine-rich loop (G-loop) Gly-X-Gly-X-X-Gly. The highly flexible G-loop can adopt various conformations, depending on the conformational state of a protein kinase and the presence of a ligand. The G-loop covers and anchors the nontransferable ATP phosphates. A survey of all human kinase sequences has shown that only Gly, Ala, or Ser occur at the first and third glycine positions (Gly11 and Gly16 in CDK2) in the G-loop (Gly11 is contained within 94% of protein kinases) and only Gly occurs at the second position (Gly13 in CDK2).[2] This indicates that replacement of this glycine is not readily tolerated.

The catalytic cleft consists of two regions: the front cleft and the back cleft. While the front cleft contains predominantly the ATP-binding site, the back cleft comprises elements important for regulation of kinase catalysis.[25] These two regions share a border formed by the β_8 strand, the N-terminus of the activation segment (A-segment) including the DFG motif,[19] and the β_3 strand on the opposite side (Figure 2). A gate between

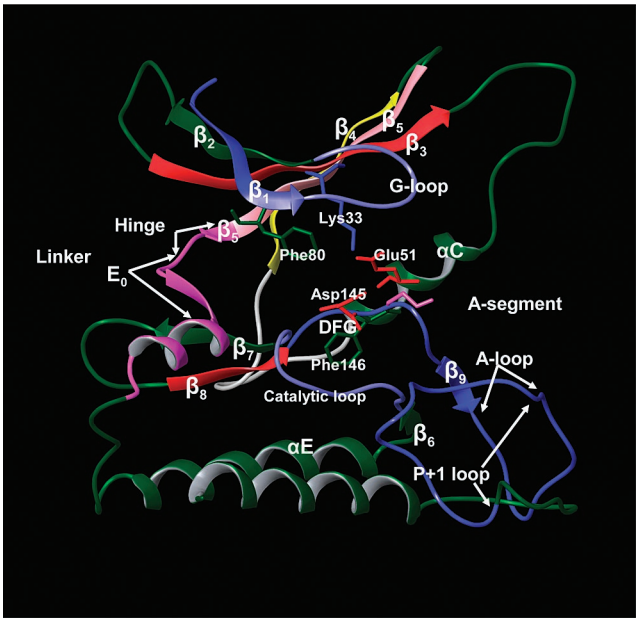

Figure 2. Ribbon representation of the catalytic cleft in the CDK2 kinase domain (PDB code 1QMZ). Important structural elements are labeled and colored. The N and the C lobes are connected with the linker (purple) that contains the hinge (a β_5 (pink) residue (Glu81) included) and the E_0 motif. The A-segment (blue) includes the DFG motif, β_9, the A-loop, and the P + 1 loop. The loop between αC and β_4 (yellow) on the back of the cleft is colored gray. Phe80 (gatekeeper) in β_5, Lys33 in β_3, Glu51 in αC and Asp145 and Phe146 in the DFG motif are labeled.

the front and the back clefts is formed by a gatekeeper residue in β_5 (Phe80 in CDK2) and a lysine in β_3 (Lys33 in CDK2). The access to the back cleft is controlled by the gatekeeper residue:[26−29] a small amino acid such as threonine or alanine at this position allows the back cleft to be accessible; a bulky gatekeeper including phenylalanine, leucine, or methionine blocks the entry of a small molecule into the back cleft through this internal gate. As another part of the gate the β_3 lysine can adopt various conformations in different protein kinase complexes.[30] This lysine conserved in all kinase enzymes is functionally important in kinase catalysis.[2] In the active state, the β_3 lysine helps to anchor the α- and β-phosphates of ATP; the lysine−ATP contact is stabilized by an ion pair formed between this residue and the catalytic glutamate residue (Glu51 in Figure 2) located nearly at the center of αC.[1]

The A-segment in the C-lobe and αC in the N-lobe are two key elements for regulation of the kinase enzymatic activity.[25] The A-segment consists of the DFG motif, the activation loop (A-loop), the P + 1 loop, and other secondary structural elements (Figure 2).[19] In a fully active state, the A-segment adopts an open conformation so that the A-loop is positioned away from the catalytic center, providing a platform for substrate binding. An active protein kinase adopts only a DFG-in conformation where the side chain of the DFG aspartate (Asp145 in CDK2) is directed into the ATP binding site and the aromatic ring of the phenylalanine (Phe146 in CDK2) is positioned in the back cleft. In the active DFG-in conformation, the aspartate is required to chelate Mg^{2+} and helps to orient the γ-phosphate for its transfer. The phenylalanine aromatic side chain in the active DFG-in motif is in contact with αC.[24] This contact in many active kinases facilitates the formation of the aforementioned Lys-Glu ion pair for the kinase catalysis.[25] A switch of the A-segment between active and inactive states, frequently coupled with αC, can significantly alter the cleft conformation.

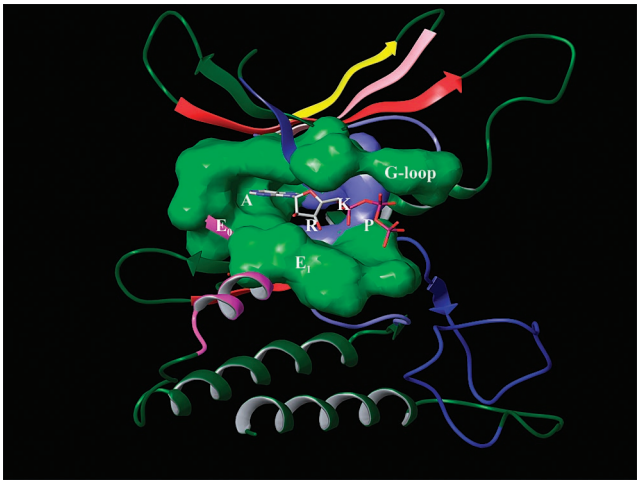

Figure 3. Molecular surface representation of the binding pockets in the front cleft (CDK2 complexed with ATP, PDB code 1QMZ). The adenine, ribose, and phosphate pockets are colored green and denoted A, R, and P, respectively. The K region is light-blue. The E_0 and E_1 regions are labeled.

In an inactive state of CDK2 as well as many other protein kinases, for example, the antiparallel strands β_6 and β_9 in Figure 2 are disrupted.[31] Importantly, while the DFG-in conformation is required for the catalysis of an active protein kinase mentioned above, this motif in inactive kinases can be DFG-in, DFG-out, or DFG-out-like.[32] In the DFG-out conformation, the Phe aromatic ring is extended into the ATP-binding site and the Asp side chain is positioned in the back cleft; the DFG backbone is significantly shifted to the ATP-binding site. A DFG-out-like motif positions the Phe and Asp side chains in a manner similar to a DFG-out one. However, its main chain is relatively close to αC compared to the DFG-out conformation, as discussed in detail later in this section.

The kinase catalytic cleft consists of distinct binding pockets. Although a pocket in different protein kinases can vary in sequence and conformation, the positions in secondary structures of pocket residues, which significantly contribute to protein−ligand interactions if the pocket is accessible for ligand binding, are highly conserved.[32] Without loss of generality, the binding pockets are elucidated using crystal structures of protein kinases including CDK2,[24] epidermal growth factor receptor (EGFR),[33,34] stem cell factor receptor (c-Kit)[35] tyrosine kinases, c-Abl (Abelson leukemia virus) tyrosine kinase,[36,37] B-Raf,[38] p38 mitogen-activated protein (MAP),[39] and Aurora A[40] serine/threonine kinases in complex with their respective ligands whose binding modes are described in detail in the next section.

Binding Pockets in the Front Cleft. The front cleft contains mainly the ATP binding site and relatively small non-ATP contact regions. As is well-documented in the literature,[6,41,42] the ATP binding site comprises the adenine, ribose, and phosphate binding pockets denoted A, R, and P in Figure 3, respectively.

The adenine binding pocket is highly hydrophobic, providing a major scaffold for ATP or inhibitor binding. The β_1−β_3 strands each provide one hydrophobic residue (Ile10, Val18, and Ala31 in CDK2, respectively) in close contact with the adenine ring from the N-lobe, whereas the loop between αC and β_4, and β_7 each contributes one from the opposite side of the adenine ring (Val64 and Leu134 in CDK2). The pocket is rimmed with the gatekeeper (Phe80 in CDK2) and the hinge (Glu81, Phe82, and Leu83 in CDK2). The first and third hinge residues are the hydrogen-bond (H-bond) providers for ATP binding shown in Figure 4. In the CDK2−ATP complex discussed above,[24] Glu81

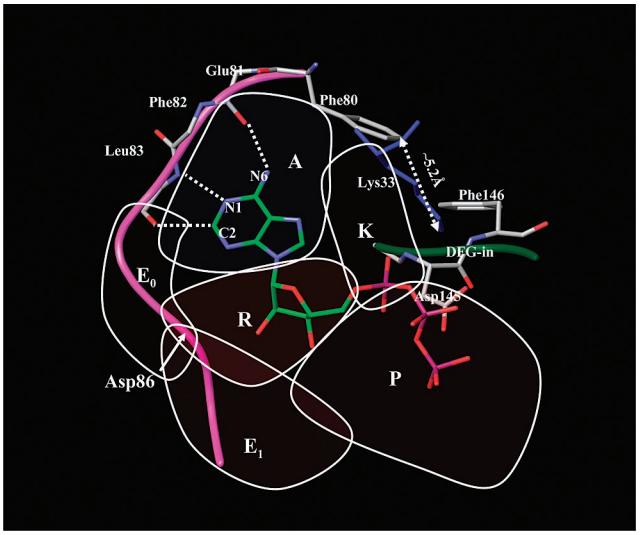

Figure 4. View of the binding pockets (A, R, P, K, E_0, and E_1 represented by the closed lines) in the CDK2 (with ATP) front cleft. The hinge residues Glue 81, Phe 82, and Leu 83 are shown only with the main chains. The three canonical H-bonds between the hinge and ATP are depicted by the dashed lines. The internal gate is ~5.2 Å wide (between the Lys33 NZ atom and the Phe80 CZ atom). Asp145 and Phe146 in the DFG-in motif are labeled. The position of Asp 84 is also shown.

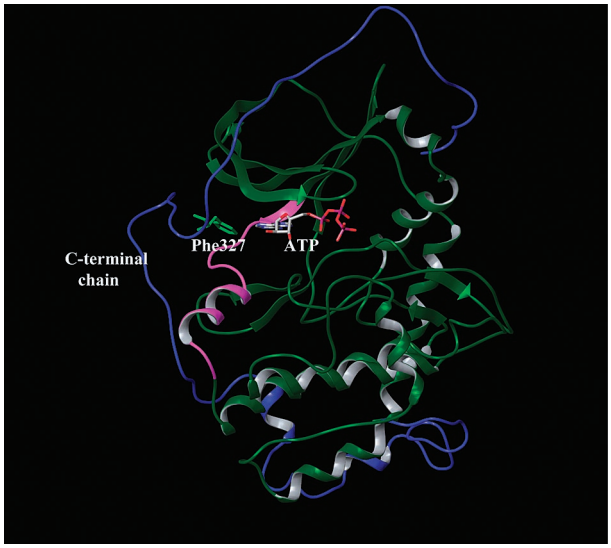

Figure 5. Ribbon representation of PKA in complex with ATP (PDB code 1ATP). Phe327, located on the C-terminal polypeptide chain (dark blue) and which folds back into the N-lobe, shields the entrance side of the adenine pocket.

accepts a H-bond from the adenine N6 atom while Leu83 donates a H-bond from its main chain nitrogen to N1 in the adenine ring and accepts a weak H-bond from the adenine C2 atom (Figure 4). Many potent small-molecule kinase inhibitors bind in the adenine pocket with one or more hydrogen bonds in a similar pattern.[42]

Although the adenine binding pocket is highly conserved in the protein kinase family, some protein kinases have specific features in this pocket. Important examples include most AGC kinase subfamily members,[21,43,44] casein kinase II (CK2),[45−49] and the Pim-1 kinase.[20] The AGC subfamily members including PKA, protein kinase B (PKB), and Rho-associated coiled−coiled containing protein kinase (ROCK) have a characteristic phenylalanine residue (Phe327 in PKA and Phe368 in ROCK) that is positioned on a C-terminal chain, which folds back into the N-lobe across the catalytic cleft seen in Figure 5 (PKA, PDB code 1ATP[44]). This residue, with an aromatic ring shielding one side of the adenine pocket, significantly contributes to the protein−ATP contact, distinguishing the adenine pocket of the AGC subfamily from others without a corresponding residue. In CK2, a bulkier residue isoleucine (Val66 in CK2) occupies the position of a smaller alanine (Ala31 in CDK2), which is conserved in many ATP-specific protein kinases.[2] This replacement and Met163 in CK2 for a leucine (Leu134 in CDK2) are important for CK2 binding to either ATP or GTP as a phosphodonor.[45−49] In addition, Ile174 in CK2 occupies the Ala144 position in β_8 of CDK2. Together, the bulky side chains of these residues make the CK2 adenine pocket smaller than that in the majority of other protein kinases responsible for the specific mode of emodin binding in CK2.[45] Pim-1 is an oncogene-encoded serine/threonine kinase. The third hinge residue is a proline (Pro123), and hence, a highly conserved H-bond provider at this position (Leu83 in CDK2) is removed.[20]

The ribose pocket consists of three hydrophobic residues (Ile10, Val18, and Leu134 in CDK2) shared with the adenine pocket, Gly11−Glu12 (backbone) in the G-loop, Asp86 and Lys89 in the linker region, and Gln131 in the catalytic loop. CDK2 numbering is used here and in the following discussion. This pocket is adjacent to a hydrophilic and solvent-exposed entrance (E_1 in Figure 3). The phosphate pocket covered by the G-loop has Lys33, the residues Asp127, Lys129, and Asn132 in the catalytic loop, and the DFG aspartate. This pocket is highly flexible, hydrophilic, and solvent-exposed particularly in an active state and is thereby believed to be less important in achieving high affinity for ligand binding.[6,41] Nevertheless, the phosphate pocket could be used to improve inhibitor physicochemical properties and gain some selectivity in lead optimization,[41,50] especially for an inactive kinase target.[51]

E_0 in Figures 3 and 4 is a region that is not used by ATP and often serves as an entrance for ligand binding. This region is frequently used to gain some selectivity in the design of protein kinase inhibitors because of its diversity in sequence and conformation.[41,42] A relatively small region (K in Figures 3 and 4) is located in the deep front pocket. This region shares the gatekeeper residue with the adenine pocket, shares the β_3 lysine and the DFG aspartate with the phosphate pocket, and contains a residue immediately preceding the DFG motif (Ala144 in CDK2). The K region is also used in kinase inhibitor design discussed later.

Binding Pockets in the Back Cleft. The binding pockets in the back cleft are non-ATP-contact. There exists a hydrophobic binding pocket in the back cleft that adjoins the adenine pocket, labeled BP-I in Figure 6. This pocket has often been used in the design of inhibitors to gain selectivity for kinase targets with a small-sized gatekeeper.[52,53] In the crystal structure of an active EGFR complexed with erlotinib (**3**) (PDB code 1M17),[33] BP-I contains Ala719 (Ala31 in CDK2), Lys721 (Lys33 in CDK2), Met742 in αC (Leu55 in CDK2), the gatekeeper Thr766 (Phe80 in CDK2), and Leu764−Ile765 (Leu78−Val79 in CDK2) in β_5. The BP-I pocket in this complex accommodates the acetylene group of the drug seen in Figure 6.

The second hydrophobic binding pocket in the back cleft is denoted BP-II in Figure 7. In an inactive form of EGFR complexed with lapatinib (**7**)[54] (PDB code 1XKK),[34] this pocket consists of the αC residue Met742 (1M17 numbering), the residues Cys751−Leu753 including the main chain of Arg752 (Val64−Leu66 in CDK2) in the loop between αC and β_4, the gatekeeper residue Thr766, Thr830 in β_8, and the DFG motif. As shown in Figure 7, BP-II is well recognized by the

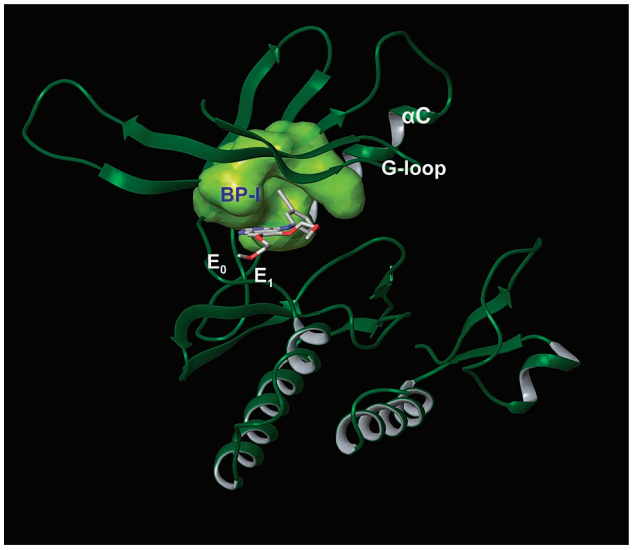

Figure 6. Molecular surface representation of BP-I in the active EGFR kinase domain complexed with erlotinib (**3**) (PDB code 1M17). The pocket is recognized by the acetylene group of **3**.

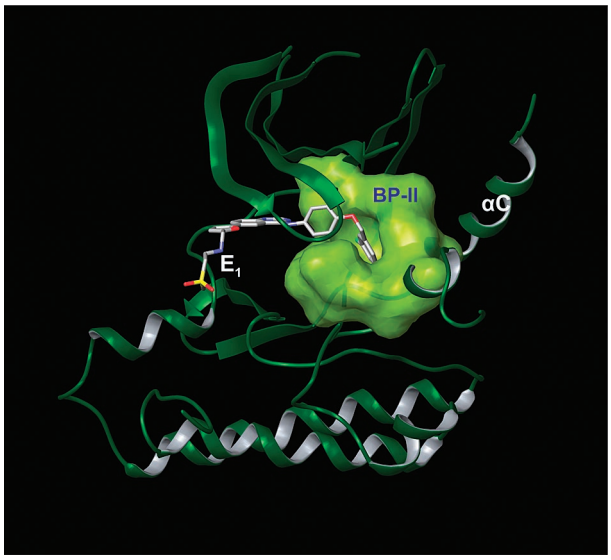

Figure 7. Molecular surface representation of BP-II in the inactive EGFR with lapatinib (**7**) (PDB code 1XKK). The 3-fluorobenzyl group of **7** binds into the pocket.

3-fluorobenzyl group of the inhibitor. The inactive EGFR as well as many other inactive protein kinases adopts a DFG-in conformation with the aspartate deviating from its active site. BP-II in this case is also referred to as the DFG-in pocket. BP-II in the active EGFR comprises the same pocket residues (except for Glu738, Figure 8) but is of smaller size. The αC helix in the inactive EGFR−lapatinib complex is shifted outward by ∼9.0 Å at its N-terminal end compared to the active structure, enlarging the inactive DFG-in pocket with the catalytic glutamate pointing out of the cleft (Figure 8).[34] Nevertheless, the topological distribution of the accessible binding pockets in this inactive DFG-in cleft is similar to the active one shown in Figure 9a.

A number of inactive protein kinases have a DFG-out conformation. The BP-II pocket with this conformation is denoted the DFG-out pocket in Figure 9b. The crystal structure of the B-Raf and sorafenib (**4**) complex (PDB code 1UWH)[38] shows that (Figure 10) the catalytic glutamate in αC (Glu500 in B-Raf) is inserted into the deep hydrophobic pocket and accepts a H-bond with its carboxylate side chain from the amide

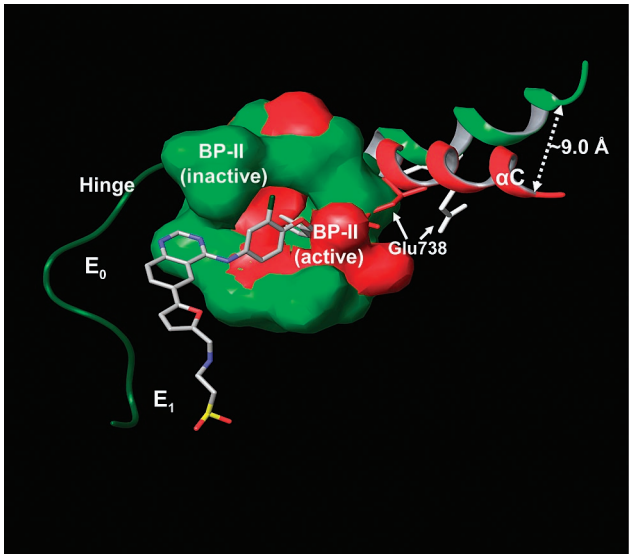

Figure 8. Superposition of the X-ray structures of the active (red) and the inactive (green) EGFRs (PDB codes 1M17 and 1XKK). The inactive αC shifts outward by ∼9.0 Å compared to the active one at its N-terminus. In the inactive form, Glu738 (gray), is directed out of the cleft, while its active counterpart (red) is positioned into the pocket. The 3-fluorobenzyl group of lapatinib (**7**) binds in inactive BP-II (green) (see Figure 7) but clashes with Glu738 and Met742 in the active pocket (red).

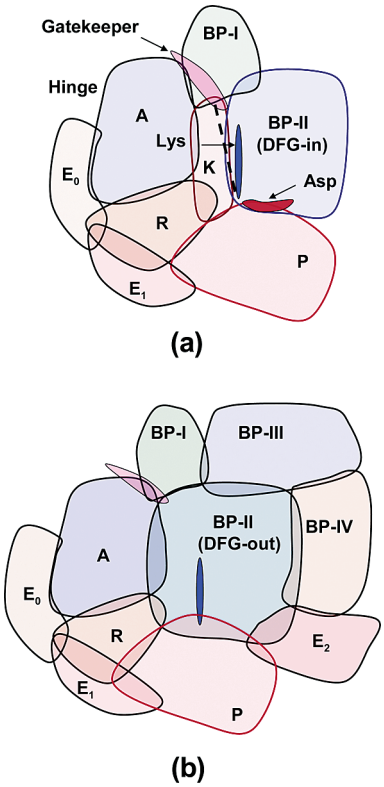

Figure 9. Topological distribution of the binding pockets in the catalytic cleft with (a) a DFG-in conformation and (b) a DFG-out conformation. The K region in (a) is merged into the DFG-out pocket in (b).

nitrogen of the inhibitor, contributing significantly to the DFG-out pocket. Another hydrogen bond forms between the carbonyl oxygen of the urea group of the drug and the main chain nitrogen of Asp593 in the DFG motif. The DFG-out pocket provides another main binding scaffold different from the adenine pocket. Similar hydrogen-bonding patterns have been observed in the

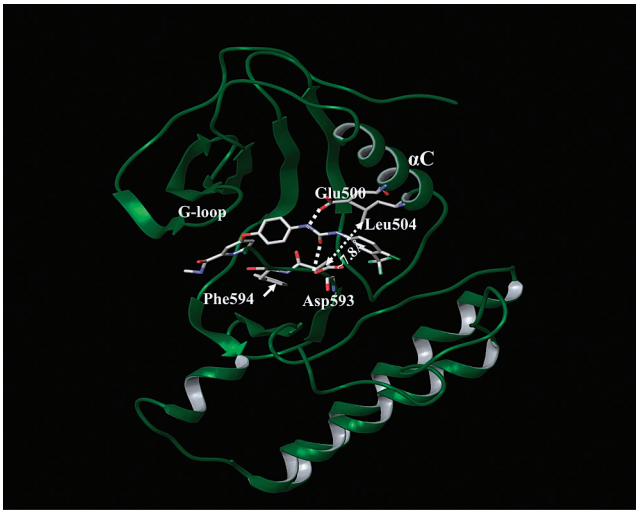

Figure 10. Ribbon representation of B-Raf in complex with sorafenib (**4**) (PDB code 1T46). In the DFG-out pocket, Glu500, accepts a H-bond with its carboxylate oxygen from the amide nitrogen of the drug molecule; the main chain nitrogen of Asp593 donates a H-bond to the carbonyl oxygen of the urea group of the inhibitor. The second internal gate in the cleft formed by Leu504 in αC and Asp593 in the DFG motif is ∼7.8 Å wide, allowing the DFG-out pocket to be open to the cleft basement (see Figure 12).

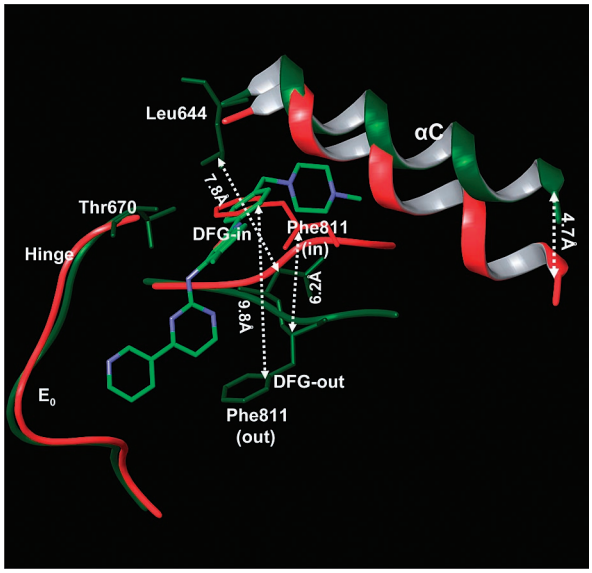

Figure 11. Conformational changes in the c-Kit binding cleft using the superposition of the inactive (dark green, DFG-out) and active (red, DFG-in) structures (PDB codes 1T46 and 1PKG). The backbone of the DFG-out Phe811 (Cα) shifts to the ATP-binding site by ∼6.2 Å and the aromatic side chain (CG) of Phe811 by ∼9.8 Å relative to their active counterparts. The inactive αC moves outward by ∼4.7 Å at its N-terminus. The gate width is ∼7.8 Å (between the CG atom of Leu 644 and the CB atom of Asp810). In addition, imatinib (**1**) clashes with Phe811 (red) in the active DFG-in conformation.

c-Abl-imatinib (**1**)[36,37] and p38 MAP-doramapimod (**8**)[39] complexes. Other protein kinases that have a similar DFG-out pocket include the insulin receptor (IRK),[55] c-Kit,[35] vascular endothelial growth factor receptor 2 (VEGFR2),[56,57] and Fms-like tyrosine kinase 3 (Flt3).[58] IRK, c-Kit, Flt3, and other receptor protein kinases share a similar mechanism of autoinhibition where a juxtamembrane domain plays an important role in the formation of the DFG-out conformation, while the inactive kinase structures in many nonreceptor tyrosine kinases including c-Abl are formed through Src homology domains SH2 and SH3. In particular, a crystallographic study has indicated that binding of the N-terminal myristoyl group into a deep hydrophobic cavity at the C-lobe of c-Abl is important for the formation of the autoinhibitory DFG-out conformation.[59] Despite the different autoinhibition mechanisms between c-Abl and c-Kit, the two inactive structures share a remarkable commonality in the catalytic cleft. As such, imatinib (**1**) is allowed to bind potently into both c-Abl and c-Kit.[35,60] Interestingly, while the DFG-out conformation in the unphosphorylated IRK as well as c-Kit is formed in the absence of ligand, the DFG-out conformations in the c-Abl-imatinib (**1**), B-Raf-sorafenib (**4**), and p38 MAP-doramapimod (**8**) complexes appear to require ligand binding.

The DFG-out conformation significantly alters the accessibility and topological distribution of the binding pockets in the cleft (see Figure 9b). In the crystal structure of the inactive c-Kit complexed with imatinib (**1**) (PDB code 1T46),[35] the aromatic side chain and the main chain of the DFG phenylalanine are shifted ∼9.8 and ∼6.2 Å to the ATP binding site, respectively, relative to their counterparts in the active conformation (PDB code 1PKG),[61] as shown in Figure 11. Similar conformational changes have been observed in other aforementioned protein kinase complexes. The back cleft with the DFG-out conformation is thus significantly enlarged, opening a gate to the basement in the C-lobe that contains the C-terminal end of the αE helix and the N-terminus of the catalytic loop, rendering the BP-III pocket in Figure 9b accessible for inbibitor binding. In the B-Raf-sorafenib (**4**) complex, BP-III contains Val503 in αC, Thr507 and Ile512 in the αC−β_4 loop, Leu566 in αE, His573 in the catalytic loop, and Gly592 in β_8; this pocket

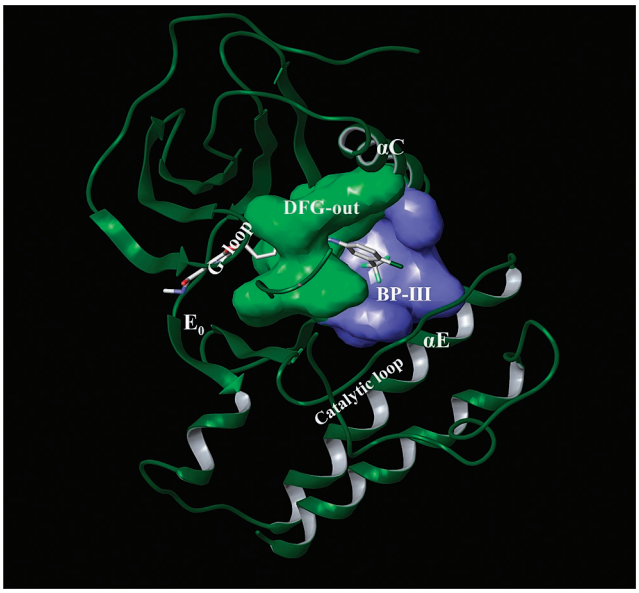

Figure 12. Molecular surface representation of BP-II (green) and BP-III (blue) in B-Raf complexed with sorafenib (**4**). The trifluoromethyl group of the drug molecule binds into the BP-III pocket.

accommodates the trifluoromethyl group of sorafenib (**4**) seen in Figure 12. A partial hydrophobic pocket BP-IV (Figure 9b) in the B-Raf complex consists of residues Val503, Leu566, and His573, which are shared with BP-III, and I8e571−Ile572 and Asp593 in the DFG motif. In the p38 MAP-doramapimod (**8**) complex, BP-III is occupied by the trimethyl substituent on the pyrazole ring, and a region (E_2 in Figure 9b) located at the side of αC is recognized by the tolyl group of the compound.

The crystal structure of Aurora A complexed with **9** (PDB code 2C6E)[22,40] reveals that the kinase enzyme adopts a DFG-out-like conformation. The gate to the C-lobe basement is ∼5.0 Å wide in the Aurora complex and is relatively small compared

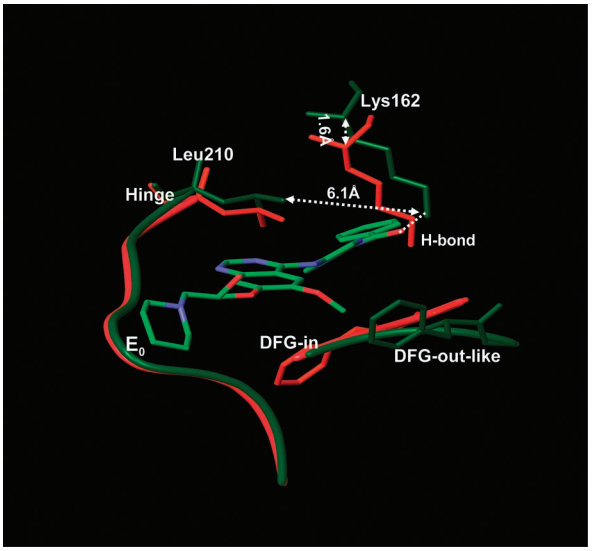

Figure 13. Conformational changes in the Aurora A cleft from the superposition of the inactive (dark green, DFG-out-like) complex with compound **9** and the active (red) structure (PDB codes 2C6E and 1OL7). Lys162 (dark green) in β_3 in the DFG-out-like form is lifted by ~1.6 Å compared to the active one. In this inactive structure, the internal gate is ~6.1 Å wide and blocks inhibitor binding into the back cleft through this gate. Nevertheless, **9** enters the back cleft through passing the border under the gate. Compound **9** clashes with Lys162 (red) in the active state.

to those (~7.8 Å) in the B-Raf and c-Kit DFG-out conformations seen in Figures 10 and 11. The C-lobe basement is therefore inaccessible for inhibitor binding. The topological distribution of the accessible binding pockets in this case is similar to that in the DFG-in conformation. Superposition of this Aurora complex[22] and the active form[62,63] indicates that αC rotates around its long axis, shifting upward and outward. Consequently, the ceiling of the N-lobe is lifted so that Lys162 in β_3 moves upward by ~1.6 Å away from its counterpart in the active form shown in Figure 13. In addition, the phenylamino group of the aminoquinazoline in the complex appears to repel the side chain of Lys162 toward αC. Together, these conformational changes allow the inhibitor to penetrate into the back cleft under, rather than through, the internal gate (6.1 Å in width) with a bulky gatekeeper leucine (Leu210 in Aurora A) shown in Figure 13.

In the X-ray structure[37] of c-Abl complexed with compound **10**[64] (PDB code 1M52), the target also adopts a DFG-out-like conformation in which, however, the DFG backbone is positioned in an active-like fashion as the A-loop adopts an open conformation that mimics the activated form. Interestingly, compound **10** is more potent than imatinib (**1**) against c-Abl although it binds in c-Abl with a lower contact surface area (913 Å^2 for compound **10**; 1251 Å^2 for imatinib) and with fewer H-bonds. Compound **10** inhibits c-Abl potently in both active and inactive states, whereas imatinib (**1**) only binds in the highly specific DFG-out conformation. A fraction of the binding free energy of imatinib (**1**) to c-Abl may be used to stabilize the A-loop conformation.

Binding Modes of Protein Kinase Inhibitors

The binding pockets in the catalytic cleft play different roles to gain binding affinity in protein kinase inhibitor design. A most reliable way to increase ligand-binding affinity is to exploit hydrophobic interactions. The burial of a methyl group in a hydrophobic pocket, for example, can contribute to the binding affinity by up to a factor of 10 at the physiological temperature.[62]

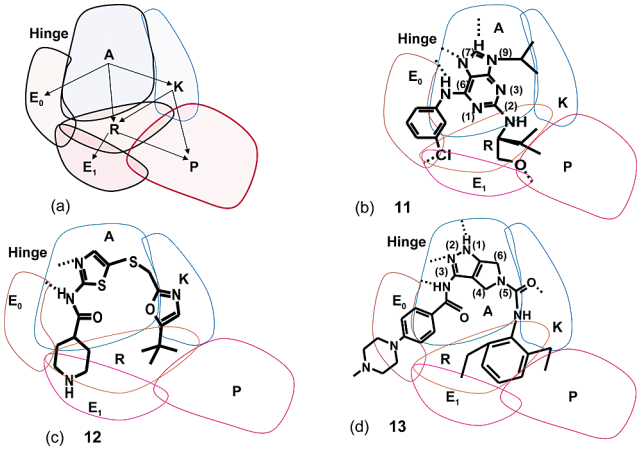

Figure 14. Two-dimensional (2D) representation of binding modes in the front cleft. (a) Schematic classification of modes of inhibitors binding in different combinations of the pockets in the front cleft. Binding modes of (b) purvalano A (**11**) in CDK2, (c)**12** in CDK2, and (d) **13** in Aurora A. In this and the following figures, a dashed line represents a hydrogen or halogen bond and the detailed descriptions of the kinase−inhibitor interactions are given in the text.

Hydrogen-bonding interaction in the hydrophobic environment, whose dielectric constant is relatively small, can significantly improve the inhibition potency of a compound. In addition, halogen bonding can increase the binding affinity estimated to be about half to slightly more than that of an average hydrogen bond.[63] By way of contrast, it is relatively difficult to utilize ionic or polar interactions to enhance inhibitor binding significantly in the hydrophilic environment because of the desolvation penalty.[64] The adenine pocket or the DFG-out pocket in the deep cleft therefore provides an important major scaffold for a core template to bind. An often used structure-based strategy is to hit a main binding pocket in the cleft with a core fragment and to decorate this core fragment with various chemical groups extended into different binding pockets. The binding modes of protein kinase inhibitors can thus be classified according to different combinations of the binding pockets recognized by inhibitors.

Modes of Inhibitor Binding in the Front Cleft. The front catalytic cleft of all kinase enzymes can be accessible for ligand binding. The vast majority of potent small-molecule inhibitors that target the front cleft use a core template to recognize the key pharmacophoric features of the adenine pocket.[68−71] The core fragment is then extended optimally into different pockets with substituted groups, as schematically classified in Figure 14a.

Significant efforts have been made in the development of small-molecule inhibitors targeting cyclin-dependent kinases. Numerous potent compounds whose binding modes cover most cases in Figure 14a have been reported in the literature.[71−74] In the following discussion, purine-based and aminothiazole-based compounds are exemplified for CDK2 inhibitors. Optimization of the purine-based compounds at the 2, 6, and 9 positions of the adenine ring to target the front cleft has been extensively studied.[75−79] The purine core can adopt multiple modes to interact with the adenine pocket. This core fragment in purvalanol A (**11**)[80,81] and other purines[76,78,82−84] adopts a similar orientation but different from that of ATP. The binding mode of **11** is shown in Figure 14b. Two canonical hydrogen bonds are formed between the purine nitrogen N7, N6 atoms and the backbone amide nitrogen, oxygen of Leu83, respectively. Purine C8 donates a weak H-bond to the carbonyl oxygen of Glu81. The 3-chloroaniline substituent extends into the E_0 region with

its phenyl group to make contact with the Phe82 aromatic side chain and the Ile10 aliphatic side chain and with its chlorine substituent in halogen bonding to Asp86. This halogen interaction leads to a ~20-fold increase in the binding affinity.[81] The substituent at the C2 position of purvalanols occupies the ribose pocket. Its *R*-isopropyl group tightly interacts with the G-loop, while the hydroxyl group forms a hydrogen bond with the backbone carbonyl oxygen of Gln131 in the catalytic loop.[80,81] Extensive efforts on a series of aminothiazole-based compounds have resulted in a potent CDK2 inhibitor, compound **12**, with the optimal pharmacokinetic properties. The X-ray structure of CDK2/cyclin E with **12** reveals the binding mode of the inhibitor.[85] As shown in Figure 14c, the main fragment aminothiazole binds in the adenine pocket with two hydrogen bonds linked to the hinge residue Leu83. The compound adopts a conformation with the *tert*-butyloxazole ring folded back to the ribose pocket. The piperidinyl ring extends toward the E_1 region. Interestingly, another aminothiazole derivative dasatinib (**6**) with an extended conformation similar to unbound **12** binds to the Src kinase back cleft in a different mode[14] (see Figure 18d).

Combinatorial optimization of 3-amino-1,4,5,6-tetrahydropyrrolo[3,4-*c*]pyrazoles has led to a potent Aurora A inhibitor, compound **13**.[86] The mode of inhibitor binding in Aurora A is illustrated in Figure 14d. The crystal structure of Aurora A in complex with **13** (PDB code 2BMC)[86] shows that the core template forms three canonical H-bonds with the two hinge residues Glu211 and Ala213 (Glu81 and Leu83 in CDK2), respectively. The benzamido substituent at the C3 position of the main fragment is directed into the E_0 region with the 4-methylpiperazin-1-yl end improving potency and aqueous solubility of the compound.[86] The N5 substituent extends into the K region, forming a hydrogen bond between its amide oxygen and the Lys162 side chain nitrogen (Lys33 in CDK2). The 2,6-disubstituted phenyl ring at the N5 substituent is positioned approximately perpendicular to the pyrrolopyrazole ring so that one ethyl substituent interacts with the G-loop. The bicyclic tetrahydropyrrolo[3,4-*c*]pyrazoles have also been developed to target CDK2 in a similar binding mode.[87]

A series of indolinone derivatives have emerged as multitargeted tyrosine kinase inhibitors.[88−92] The indolinones[88,89] including compound **14** have been crystallized within the catalytic domain of fibroblast growth factor receptor (FGFR) tyrosine kinase. In the crystal structure of FGFR1 in complex with **14**,[89] the oxindole core binds into the adenine pocket with two hydrogen bonds between the oxindole N1 atom and the Glu562 carbonyl oxygen and between the oxindole O2 atom and the Ala564 amide nitrogen (Figure 15a). The pyrrole ring is covered by Leu484 in β_1 and Tyr563 in the hinge, whereas the propionic acid substituent at the C3′ position occupies the ribose pocket and interacts with Asn568 with a hydrogen bond in the E_1 region. In addition, O2 of the oxindole core forms an intramolecular H-bond with N1′ on the pyrrole ring, helping to stabilize the planar conformation of the compound. While **14** has not shown promising results in clinical trials,[93] the indolinone derivative sunitinib (**5**) (see Figure 15b) is reasonably well tolerated[94] and was recently approved for the treatment of gastrointestinal stromal tumor (GIST) and advanced kindey cancer.

Fasudil (**15**), a vasodilator used for the treatment of cerebral vasospasm, is an isoquinoline-based inhibitor of ROCK.[95−98] The crystal structure of ROCK-I complexed with fasudil (PDB code 2ESM)[21] shows that the isoquinoline core binds in the adenine pocket with two H-bonds anchored to the hinge (Figure 15c); the isoquinoline nitrogen accepts a H-bond from the Met156 backbone amide nitrogen, and C1 donates a weak H-bond to the Glu154 main chain carbonyl oxygen. The homopiperazine occupies the ribose binding pocket, displayed in Figure 15c. Hydroxyfasudil (**16**), an active metabolite of fasudil, is a more potent and selective inhibitor of ROCK than the parent compound.[95] In the ROCK−hydroxyfasudil complex (PDB code 2ETK),[21] the isoquinolinone core occupies the adenine pocket in an orientation reverse to that of fasudil so that the carbonyl oxygen of the isoquinolinone accepts a H-bond from the Met156 amide nitrogen while the protonated nitrogen donates a H-bond to Glu154 (Figure 15d). The homopiperazine ring of hydroxyfasudil (**16**) extends into the phosphate pocket with its secondary amine hydrogen bonding to the Asp216 side chain oxygen.

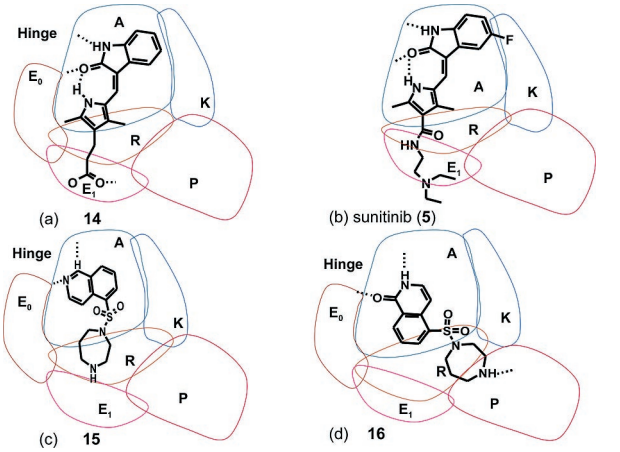

Figure 15. Binding modes of (a) **14**, (b) sunitinib (**5**) in FGFR1, (c) fasudil (**15**), and (d) hydroxyfasudil (**16**) in ROCK in the 2D representation.

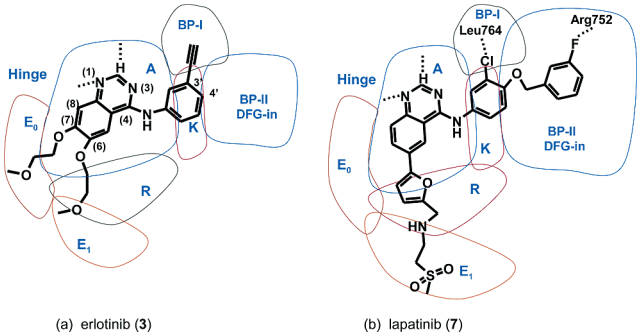

Figure 16. Binding modes of (a) erlotinib (**3**) in the active EGFR and (b) lapatinib (**7**) in the inactive EGFR in the 2D representation.

Modes of Inhibitor Binding in the Front and Back Clefts. In the 4-anilinoquinazoline class of compounds, gefitinib (**2**),[10] erlotinib (**3**),[11] and lapatinib (**7**)[99] are potent and selective inhibitors of EGFR. The crystal structures for EGFR in complex with erlotinib (**3**) (PDB code 1M17)[33] and lapatinib (**7**) (PDB code 1XKK)[34] reveal the binding modes of the compounds. As discussed earlier, erlotinib (**3**) binds in the active form of EGFR whereas lapatinib (**7**) targets the inactive enzyme. In both complexes seen in Figure 16, N1 of the quinazoline core accepts a H-bond from the amide nitrogen of Met769 (numbering used in 1M17) in the hinge. The quinazoline C2 atom donates one weak H-bond to the carbonyl oxygen of the hinge residue Glu767 (Glu81 in CDK2). In EGFR complexed with erlotinib (**3**), the acetylene moiety at the C3 position of the phenyl ring is directed into the BP-I pocket, significantly improving the compound selectivity. As shown in Figure 16a, the C6 and C7

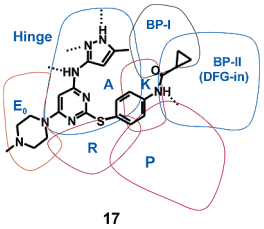

Figure 17. Mode of compound **17** binding in the active conformation (DFG-in) of c-Abl.

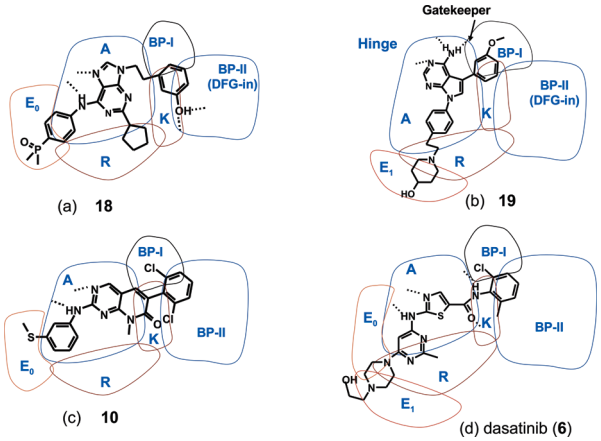

Figure 18. Modes of the dual Src and c-Abl inhibitors (a) **18** binding in Src, (b) **19** in Src, (c) **10** in c-Abl with a DFG-out-like conformation and (d) dasatinib (**6**) in the active c-Abl.

substituents extend into the entrance regions. In the EGFR−lapatinib (**7**) complex, the 3′-chloroaniline group oriented into the BP-I pocket forms a halogen bond with the carbonyl oxygen of Leu764 in β_5 (1M17 numbering). The 3-fluorobenzyl group extends in the DFG pocket with halogen bonding to the carbonyl oxygen of Arg752. The C6 substituent is directed into the E_1 region.[34]

Compound **17** is an Aurora kinase inhibitor[100] and also inhibits potently the active form of c-Abl.[101] The X-ray structure of the Abl H396P mutant complexed with **17** discloses a Y-shaped binding mode.[102] In this mode, a pyrimidine fragment is located at the fork, the aminomethylpyrazole group at one arm is anchored to the hinge with three ATP-type hydrogen bonds, and the methylpiperazine base extends into the E_0 region, as shown in Figure 17. The second phenyl-substituent arm directs its cyclopropyl terminus into the DGF pocket through the ribose pocket, the K region, and the internal gate. In this arm, the amide nitrogen donates a H-bond to the side chain oxygen of the DFG aspartate; the phenyl ring is engaged in an aromatic−aromatic interaction with Tyr253 in the G-loop.

Small-molecule compounds with dual inhibitory activity against c-Abl and Src are especially attractive in the development of second-line inhibitors to thwart imatinib-resistant mutations.[103] Compounds **18**, **19**, **2**, and dasatinib (**6**) all are dual inhibitors of Src and c-Abl, whose binding modes are elaborated upon in the following discussion. **18** is a 2,6,9-trisubstituted purine-based compound,[104] the X-ray complex of which with an active Src shows the mode of inhibitor binding illustrated in Figure 18a.[104,105] The Met341 (Src numbering[106]) backbone nitrogen and oxygen form two canonical H-bonds with N7 and N6 (see numbering in Figure 14b) of **18**, respectively, similar to that of purvalanol A (**11**) binding in CDK2 as discussed earlier (Figure 14b). However, the major difference occurs at the purine N9 position; namely, the N9 substituent, a relatively large 3-hydroxyphenethyl group, penetrates into the

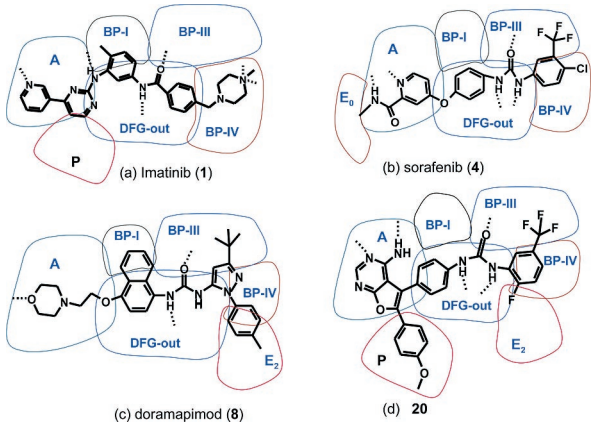

Figure 19. Binding modes of (a) imatinib (**1**) in c-Abl, (b) sorafenib (**4**) in B-Raf, (c) doramapimod (**8**) in p38 MAP, and (d) **20** in VEGFR2, all of which are in the DFG-out conformation.

DFG pocket in the back cleft with the hydroxyl group hydrogen-bonding to Glu310 and Asp404. This substituent is a key structural component, significantly increasing the inhibitor binding affinity.[105] The cyclopentyl group at the purine C2 position occupies the ribose pocket, and the C6 anilino substituent extends toward the E_0 region. The substituted 5,7-diphenylpyrrolo[2,3-*d*]pyrimidines including compound **19** are potent inhibitors of Src and Abl.[107] The X-ray structure of the Src kinase domain in complex with **19** (PDB code 1YOL) demonstrates the binding mode of the inhibitor.[108] Three H-bonds are formed between the pyrrolopyrimidine core and two hinge residues, Glu341 and Met343, and the gatekeeper residue Thr340, respectively. The methoxyphenyl substituent penetrates into the back cleft with the methoxyl group occupying the BP-I pocket and with the phenyl ring binding in the DFG-in pocket. The N5 substituent extends into the E_1 region. The inhibitor binding mode is depicted in Figure 18b.

The pyrido[2,3-*d*]pyrimidine-based inhibitors have been developed with specificity for tyrosine kinases.[64,109] A member of this class, compound **10**, is a dual Src and c-Abl inhibitor. The crystal structure of the c-Abl−**10** complex (PDB code 1M52)[37] shows that the aminopyridopyrimidine core forms two canonical hydrogen bonds with the hinge Met318. One chloro substituent of the dichlorophenyl group is positioned in BP-I, while another chloro group with the phenyl ring occupies the DFG pocket. The thiomethyl substituent at the opposite end of the inhibitor extends into the E_0 region (Figure 18c). Dasatinib (**6**),[14] a recently approved drug for adults with CML who become resistant to imatinib (**1**), is an aminothiazole-based Abl and Src inhibitor. In the c-Abl−drug complex,[14] the inhibitor binds to the back cleft in a mode similar to that of compound **10**; the 2-chloro-6-methylbenzamide group inserts into the BP-I and DFG pockets (Figure 18d). The aminothiazole core adopts a hydrogen-bonding pattern similar to that seen in the CDK2−**12** complex in Figure 14c.[85] Two more hydrogen bonds are formed between the compound amide nitrogen and the hydroxyl oxygen of the gatekeeper residue Thr315 and between the inhibitor amide oxygen and the Lys271 side chain. The substituted pyrimidine ring occupies the E_0 region, while the hydroxyethylpiperazine group extends out of the binding cleft.

Imatinib (**1**),[36,37] sorafenib (**4**),[38] and doramapimod (**8**)[39] bind into c-Abl, B-Raf, and p38 MAP, respectively, in a similar mode shown in Figure 19a−c. As mentioned earlier, the diarylamide of imatinib (**1**) and the diarylurea of sorafenib (**4**) and doramapimod (**8**) interact with the DFG-out pocket. In the c-Abl−imatinib (**1**) complex[37] (Figure 19a), the 2-aminopyrimidine

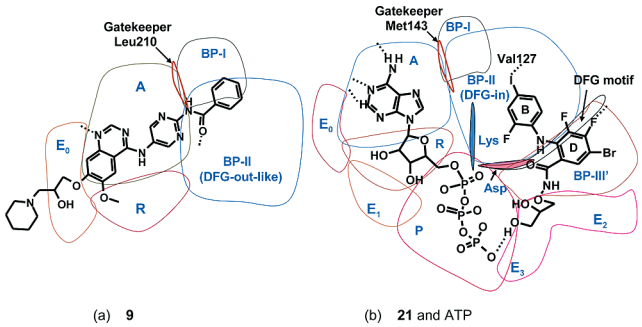

Figure 20. (a) Mode of **9** binding in Aurora A with the DFG-out-like conformation, penetrating into the back cleft through passing under the internal gate. (b) Modes of **21** and ATP binding in the MEK1 catalytic cleft. **21** binds in MEK1 through the E_2 entrance at the αC side.

fragment and the attached pyridine ring occupy the adenine pocket; the pyridine nitrogen accepts a H-bond from the main chain amide of the hinge residue Met318, and the 2-amino nitrogen donates a H-bond to the side chain oxygen of the gatekeeper Thr315. In Figure 19a, the methyl group at the central phenyl ring inserts into hydrophobic pocket BP-I, whereas the methylpiperazinyl ring penetrates into the partially hydrophobic BP-IV pocket. In B-Raf complexed with sorafenib (**4**)[38] (Figure 19b), the trifluoromethyl substituent is directed into BP-III, while the chlorophenyl group is inserted into BP-IV. At the opposite end of the inhibitor, the pyridylamide group occupies the adenine pocket, interacting with three aromatic residues, Trp530, Phe582, and Phe594, and forming two H-bonds between the pyridyl ring nitrogen and the amide nitrogen of the drug and between the Cys531 main chain amide and oxygen. The methyl end group extends toward the E_0 region. In p38 MAP complexed with doramapimod (**8**)[39] (Figure 19c), the ethoxymorpholine group binds in the adenine pocket with a H-bond between the morpholine oxygen and the backbone amide of the hinge residue Met109, while the *tert*-butyl group at the pyrazole ring is positioned in the BP-III pocket. As mentioned in the previous section, the *tert*-butyl group on the pyrazole ring is positioned in the BP-III pocket, whereas the tolyl substituent is directed into the E_2 region. Intriguingly, the significantly bulky pyrazole end of doramapimod (**8**) suggests that it could be energetically favorable for the compound to enter the back cleft through this region.

A class of the 4-aminofuoro[2,3-*d*]pyrimidine derivatives have been discovered as potent VEGFR2 inhibitors.[56] The binding mode of one potent compound **20** in this class has been demonstrated in the X-ray structure of the VEGFR2 complex (PDB code 1YWN).[56] Remarkably, the inhibitor includes two core templates, a fuoropyrimidine and a diarylurea moiety, that occupy the adenine and DFG-out pockets of the target, respectively. As illustrated in Figure 19d, the aminopyrimidine group of the fuoropyrimidine core is anchored to the hinge with two ATP-type H-bonds, whereas the 6-aryl substituent extends into the phosphate binding pocket. The diarylurea core occupies the DFG-out pocket with the attached trifluoromethyl group binding in the BP-III pocket and with the 2-fluoro substituent directed toward the E_2 region.

Most of the inhibitors, which have been observed to bind in both the front and back clefts in X-ray structures, penetrate into the back cleft through the internal gate formed by a small gatekeeper residue. However, the crystallographic study of Aurora complexed with **9** reveals a novel mode by which the inhibitor occupies the deep cleft displayed in Figure 20a.[22,40] In this crystal complex, the enzyme adopts a DFG-out-like conformation, as mentioned in the previous section. While the quinazoline fragment binds in the adenine pocket in a fashion similar to that in the EGFR−erlotinib (**3**) complex seen in Figure 16a, the pyrimidine ring interacts with the DFG phenylalanine aromatic ring and with the gatekeeper Leu210 at the opposite side. Most importantly, the phenylamide substituent is inserted into the DFG pocket through passing under the internal gate.

The crystal structures of truncated forms of both MEK1 (MAP kinase kinase 1) and MEK2 complexed with MgATP and, respectively, with inhibitors **21** and **22** have been determined.[110] The MEK1−**21** complex shows that the activation loop adopts a two-turn α-helical inactive conformation (Gln221−Phe223 are disordered). Ile141 in β_5, Leu115 in αC, the DFG motif, and Ser212−Met219 in the A-loop generate a new half-opened binding pocket (BP-III′ in Figure 20b), occupied by the D ring of the inhibitor. A hydrogen bond is formed between the 4-fluoro substituent of the D phenyl ring and the backbone amide of Ser212. The B phenyl ring penetrates into the DFG pocket. A halogen bond is formed between the 4-iodine atom and the main chain carbonyl oxygen of Val127. The hydroxamate side chain of **21** extends into the E_2 region formed by the G-loop tip (Asn78−Gly79) and a part of the A-loop (Met219−Ala220). The mode of ATP binding in MEK1 is also shown in Figure 20b for comparison. In the MEK2 complex with **21**, the inhibitor binds into the enzyme in the same mode.[110]

Specificity of Binding Pockets and Selectivity of Protein Kinase Inhibitors

Inactivation of a disease-relevant protein kinase through inhibitor binding in the catalytic cleft raises the issue of how to achieve selectivity of an inhibitor against the intended target over more than 500 other family members. Different selectivity profiles are required for protein kinase inhibitors depending on their intended clinical uses. While treatment of a nonmalignant disease requires a higher degree of selectivity, multitargeted kinase inhibitors may be beneficial to treat human malignancy either in overcoming its heterogeneity[7] or in the extension of drug clinical use.[111] For example, sorafenib (**4**), which has been approved for the treatment of patients with advanced renal cell carcinoma, inhibits the Raf kinases[12] as well as other protein kinases including VEGFR2 and PDGFR-β.[112] It is the first kinase drug that targets both RAF/MEK/ERK signaling pathway to block the tumor cell proliferation and the VEGFR2/PDGFR-β signaling cascade to inhibit the tumor angiogenesis. Inhibition of angiogenesis is believed to play an important role in the drug's success because kidney tumors are especially vascularized. Imatinib (**1**) originally designed to inhibit c-Abl for the treatment of chronic myelogenous leukemia (CML) has been found to block the c-Kit activity as well. This finding has extended the imatinib's use for patients with GIST. Furthermore, a drug-resistant mutant of a kinase target is generally more efficient in regulation of its catalysis and less specific for inhibitor binding than the unmutated form.[32] Therefore, design of somewhat more promiscuous second-line small-molecule inhibitors to target the mutated kinase isoforms is necessary. Whether the side effects of a drug candidate resulting from its promiscuity can be accepted eventually depends on the clinical tolerance. Sunitinib (**5**) approved for the treatment of patients with GIST resistant to imatinib (**1**) is a multitargeted tyrosine kinase inhibitor that blocks efficaciously tyrosine kinases including c-Kit, VEGFR, Flt3, and PDGFR.[90,94] Dasatinib (**6**), a second-line drug to outwit imatinib-resistant CML, inhibits a significant number of tyrosine kinases in the nanomolar range.[101]

The optimal selectivity profile of a promising inhibitor, however, must exclude off-targeted kinases whose activities are

critical for normal cell function. For example, GSK-3 is a multifunctional serine/threonine kinase and serves as a key regulator involved in many signaling pathways. Off-target inhibition of this enzyme could lead to malignancy.[113] Because there are a large number of important protein kinases in human cells, selectivity has proven to be a significant challenge in a kinase drug discovery program. Nevertheless, despite overall conservation in sequence and conformation, the binding pockets in the catalytic cleft have distinct features that determine the specificities for at least a subset of protein kinases. Molecular recognition of these specificity determinants is of great help in the design of an inhibitor selectivity profile. On the basis of the available crystal structures of protein kinases, the specificities of the binding pockets can be determined and classified, as exemplified below.

Molecular Recognition of Specificities of the Front Cleft. ROCK is a serine/threonine protein kinase that plays a potential role in several neurological disorders including spinal-cord injury, stroke, Alzheimer's disease, neuropathic pain, and multiple sclerosis.[98] Design of ROCK inhibitors to acheive a high degree of selectivity over functionally important protein kinases is essential for therapeutic use. For example, the catalytic clefts of ROCK and PKA as two members of the AGC subfamily are very similar. To avoid inhibition of PKA by a ROCK inhibitor could be crucial because PKA is involved in many signal transduction pathways.[21] Compound **23** is a dimethylated derivative of **15** and is ∼50-fold selective for ROCK over PKA. The X-ray structures of this inhibitor complexed with ROCK-I (PDB code 2ETO)[21] and PKA (PDB code 1Q8U)[114] show that four inhibitor-contact residues, Ile82 in β_1, Met156 in the hinge, Asp160 in the E_0 region, and Ala215 in β_8 in ROCK, are different from their PKA courterparts Leu49, Val123, Glu127, and Thr183. These residue variations, particularly the Ala215Thr exchange, are the major contributors to the selectivity of **23**. The crystal structure of the ROCK complex also shows that the inhibitor tightly interacts with Phe368. As discussed earlier (Figure 5), this residue is a specificity determinant for most AGC kinases and contributes significantly to the inhibitor selectivity against ROCK over protein kinases in other subfamilies.

E_0 in the front cleft, which contains a non-ATP contact region, can be exploited to gain binding selectivity, as mentioned previously (Figure 4). The recently developed compound **24** is ∼160-fold selective for CDK2 over GSK-3β.[115] Such selectivity is important in the design of CDK2 inhibitors because CDK2 and GSK-3β are therapeutical antagonists and often share similarities in their small-molecule inhibition profiles.[116] The structural analysis demonstrates that the position of Asp86 in CDK2 (Figure 4) is occupied by Thr138 in GSK-3β. This replacement in the E_0 region, which interferes with the interaction between the residue and the sulfonamide group of **24**, reduces the affinity of inhibitor binding to GSK-3β, significantly improving the selectivity of the inhibitor against CDK2 over GSK-3β.[115] The chloro group of **11** interacts with Asp86 of CDK2 with a halogen bond (see Figure 14b), resulting in a ∼20-fold enhancement of the binding affinity, while removal of this group has no effect on Src inhibitory potency owing to the occupancy of a serine at this position in Src.[105] There exists an asparagine at the CDK2 Asp86 position in the E_0 region of FGFR1 and Flk-1 (Asn568 in FGFR and Asn921 in Flk-1). The propionic acid side chain of **14** (Figure 15a) forms a hydrogen bond with this asparagine, leading to the inhibitor selectivity for FGFR1 as well as Flk-1.[89] The N-terminuses of E_0 in the p38 α and β isoforms are occupied by a glycine residue. This small residue allows a peptide flip between Met109 and Gly110, while the γ isoform and other MAP kinases have bulkier residues in this position, blocking such a peptide flip. This subtle conformational change accounts for the selectivity of the quinazolinone and pyridolpyrimidine inhibitors against the p38 α and β isoforms over c-Jun N-terminal kinase and ERKs.[117] The Aurora family comprises three serine/threonine protein kinases, Aurora A, B, and C, which are key mitotic regulators that have emerged as attractive targets for anticancer therapy.[69,118] Thr217 in the E_0 region of Aurora A differs from its counterpart, Glu177 of the Aurora B isoform. It is believed that a 30-fold selectivity of **17** against Aurora A over Aurora B could be attributed to this variation.[69] Most likely, the bulkier side chain of Glu177 is energetically unfavorable for **17** binding to Aurora B compared to Aurora A.

Molecular Recognition of Specificities of the Back Cleft by Inhibitor Binding through Passing the Internal Gate. About 75% of all human protein kinases have a bulky gatekeeper residue such as phenylalanine, leucine, or methionine preventing compound intrusion into the back cleft through the internal gate. As discussed in the previous section, erlotinib (**3**) and lapatinib (**7**) exploit the threonine gatekeeper to penetrate the EGFR back cleft through passing this gate. While lapatinib (**7**) is a potent dual inhibitor of the inactive EGFR and its isoform ErbB-2, erlotinib (**3**) inhibits the active EGFR but not ErbB-2 although the kinase domains of EGFR and ErbB-2 are highly homologous (88% identical in sequence).[33,34] Erlotinib (**3**) is devoid of ErbB-2 inhibitory activity most likely because of the inability of ErbB-2 to adopt an active conformation as observed in the apo and EGFR−erlotinib (**3**) structures.[34] While erlotinib (**3**) binds in the active EGFR tightly, the drug would be packed loosely in the inactive form of the enzyme because the back cleft of the inactive conformation is enlarged owing to the outward rotation of αC (Figure 8).

The DFG-out conformation is an important specificity determinant for a subset of protein kinases. Imatinib (**1**) targets the multiple inactive tyrosine kinases including c-Abl, c-Kit, and PDGFR with a similar DFG-out conformation. Sorafenib (**4**) recognizes the DFG-out conformation of protein kinases including B-Raf (Figure 10), VEGFR2, and PDGFR-β. The DFG-out conformation in p38 MAP kinase is highly specific for doramapimod (**8**) binding, as discussed previously (Figure 19c). Inactive IRK also adopts a DFG-out conformation but with a bulky methionine gatekeeper. Src tyrosine kinases have a threonine gatekeeper, and the pocket residues are markedly reminiscent of those contacted by imatinib (**1**) in c-Abl. An inactive Src kinase, however, adopts a DFG-in conformation that blocks drug binding.

Molecular Recognition of a Unique Route To Bind in the Back Cleft. MEK1 and MEK2 are dual-specificity tyrosine/threonine protein kinases, playing a pivotal role in the activation of ERK in the Raf/MEK/ERK signaling pathway. Both enzymes have a bulky methionine hindering the entry of an inhibitor through the internal gate. However, inhibitors **21** and **22** bind in the back clefts of MEK1 (Figure 20b) and MEK2 through the entrance E_2 as discussed previously. This mode of inhibitor binding is highly specific. Their analogues, compounds **25** (PD184352, CI-1040) and **26** (Figure 21), most possibly bind in the same fashion to achieve a high degree of selectivity.[70] Currently, **25** and **26** are in clinical development.

The Aurora kinases have a bulky leucine gatekeeper that blocks compound binding into the back cleft through the internal gate, as discussed previously. Nevertheless, the quinazoline-based inhibitors including **9**[69,118] recognize the DFG-out-like

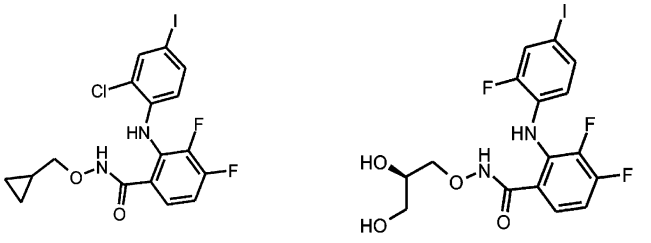

Figure 21. Structural formulas of compounds **25** and **26**.

conformation to penetrate into the back cleft. In this highly specific conformation, the N-lobe is raised upward so that the compound is able to pass the border under the gate to occupy the back cleft (Figure 13).

Concluding Remarks and Perspectives

Successful development of a kinase drug depends significantly on the choice of a suitable target. The qualification of a protein kinase as a therapeutic target is not straightforward.[5,119] A useful consideration in antitumor kinase drug discovery is that a target plays a critical role in the neoplastic pathogenesis mostly through activating oncogenic mutations.[120,121] This has been demonstrated in the examples including Raf,[38] whose oncogenic mutations are critical promoters for human malignancies. EGFR overexpression is often observed in non-small-cell lung cancer (NSCLC).[122] With the encouraging results from the early clinical trials, the large-scale, randomized, double-blind phase II trials on gefitinib (**2**) have shown that 10% of patients with NSCLC treated with the inhibitor have responded. Responses have been shown more frequently in female and in nonsmokers. The FDA approval of the drug was based on the response rate of patients with locally advanced or metastatic NSCLC after failure of both platinum-based and docetaxel chemotherapies and based on the favorable safety profile.[123] Point mutations in the EGFR kinase domain in the subgroup of patients with NSCLC reponding to the gefitinib (**2**) treatment have been detected, providing evidence for the target validation and a possible way to select patients.[122] A survey of clinical trials with 101 kinase inhibitors has shown that a total of 36 targets have been identified to be associated with 48 distinct clinical indications.[124] Although the best validation of a target is clinical efficacy and safety data, target validation at the earliest possible stage in a drug discovery program is necessary to minimize costly failures. Detailed knowledge of a kinase target can in turn help identify and optimize drug leads efficiently.

Optimization of the physicochemical properties of lead compounds to achieve an adequate pharmacokinetic (PK) and pharmacodynamic (PD) profile is essential for the success of a drug candidate in clinical development. Poor PK properties and toxicity are the major reasons for attrition in drug development processes. Small-molecule protein kinase inhibitors that bind into the catalytic domain must enter the diseased cells through different routes of administration to inhibit their targets. Oral bioavailability and other important PK properties of a kinase inhibitor are related to its physicochemical features including molecular size, hydrophobicity, hydrophilicity, hydrogen-bonding,[125−127] and others associated with active transport.[128] Because of the complexity of the action of an organism on the metabolic outcome of a drug molecule, a quantative prediction of PK properties against the compound structure presents a challenge.[129,130] Particularly small-molecule protein kinase compounds have relatively high molecular weight and calculated log *P* values compared to the average of other types of compounds in clinical development.[124]

Crystal structures of protein kinases provide a rational basis for design of potent and selective kinase inhibitors. Crystallographic studies, however, are limited at the qualitative level of description. Computational methods including virtual docking[131] can be helpful in inhibitor design. Although significant challenges remain, particularly associated with current scoring and ranking of docked compounds,[132,133] the molecular docking and other computer-aided approaches have become routine tools in targeted drug discovery.

Acknowledgment. I thank Professor David N. Beratan, Drs. Adnan M. M. Mjialli, Robert Andrews, Robert Rothlein, Edward Tian, Stephen Davis, David Jones, Ramesh Gopalaswamy, Zengbiao Li, Elizabeth Guo, and Brian Grella for helpful discussions. The constructive comments of Dr. William J. Greenlee are gratefully acknowledged.

Biography

Jeffrey Jie-Lou Liao received his B.S. degree in Chemistry at University of Science and Technology of China (USTC) and his Ph.D. degree in Physical and Computational Chemistry at USTC. He became an Associate Professor in Chemical Physics at USTC 3 years later. He had worked in the field of computational and theoretical chemistry and biophysics at Duke University before he joined TransTech Pharma, Inc. in 2005, where he has been developing methods to predict flexible structures of proteins with multiple conformations and to design potent and selective inhibitors for various targets. He has also applied a wide variety of in silico tools to aid in drug design and discovery.

References

(1) Hanks, S. K.; Hunter, T. Protein kinases 6. The eukaryotic protein kinase superfamily: kinase (catalytic) domain structure and classification. *FASEB J.* **1995**, *9*, 576−596.
(2) Manning, G.; Whyte, D. B.; Martinez, R.; Hunter, T.; Sudarsanam, S. The protein kinase complement of the human genome. *Science* **2002**, *298*, 1912−1916, 1933−1934.
(3) Cohen, P. Protein kinases, the major drug targets of the twenty-first century? *Nat. Rev. Drug Discovery* **2002**, *1*, 309−315.
(4) Noble, M. E. M.; Endicott, J. A.; Johnson, L. N. Protein kinase inhibitors: insights into drug design from structure. *Science* **2004**, *303*, 1800−1805.
(5) Weinmann, H.; Metternich, R. Drug discovery process for kinase inhibitors. *ChemBioChem* **2005**, *6*, 455−459.
(6) Kéri, G.; Orfi, L.; Eros, D.; Hegymegi-Barakonyi, B.; Szántai-Kis, C.; Horváth, Z.; Wáczek, F.; Marosfalvi, J.; Szabadkai, I.; Pató, J.; Greff, Z.; Hafenbradl, D.; Daub, H.; Müller, G.; Klebl, B.; Ullrich, A. Signal transduction therapy with rationally designed kinase inhibitors. *Curr. Signal Transduction Ther.* **2006**, *1*, 67−95.
(7) Stadler, W. M. New targets, therapies, and toxicities: lessons to be learned. *J. Clin. Oncol.* **2006**, *24*, 4−5.
(8) Zimmermann, J.; Buchdunger, E.; Mett, H.; Meyer, T.; Lydon, N. B. Potent and selective inhibitors of the Abl-kinase: Phenylaminopyrimidine (PAP) derivatives. *Bioorg. Med. Chem. Lett.* **1997**, *7*, 187−192.
(9) Druker, B. J.; Tamura, S.; Buchdunger, E.; Ohno, S.; Segal, G. M.; Fanning, S.; Zimmermann, J.; Lydon, N. B. Effects of a selective inhibitor of the Abl tyrosine kinase on the growth of Bcr-Abl positive cells. *Nat. Med.* **1996**, *2*, 561−566.
(10) Barker, A. J.; Gibson, K. H.; Grundy, W.; Godfrey, A. A.; Barlow, J. J.; Healy, M. P.; Woodburn, J. R.; Ashton, S. E.; Curry, B. J.; Scarlett, L.; Henthorn, L.; Richards, L. Studies leading to the identification of ZD1839 (Iressa): an orally active, selective epidermal growth factor receptor tyrosine kinase inhibitor targeted to the treatment of cancer. *Bioorg. Med. Chem. Lett.* **2001**, *11*, 1911−1914.
(11) Moyer, J. D.; Barbacci, E. G.; Iwata, K. K.; Arnold, L.; Boman, B.; Cunningham, A.; DiOrio, C.; Doty, J.; Morin, M. J.; Moyer, M. P.; Neveu, M.; Pollack, V. A.; Pustilnik, L. R.; Reynolds, M. M.; Sloan, D.; Theleman, A.; Miller, P. Induction of apoptosis and cell cycle arrest by CP-358,774, an inhibitor of epidermal growth factor receptor tyrosine kinase. *Cancer Res.* **1997**, *57*, 4838−4848.
(12) Lowinger, T. B.; Riedl, B.; Dumas, J.; Smith, R. A. Design and discovery of small molecules targeting Raf-1 kinase. *Curr. Pharm. Des.* **2002**, *8*, 2269−2278.

(13) Sun, L.; Liang, C.; Shirazian, S.; Zhou, Y.; Miller, T.; Cui, J.; Fukuda, J. Y.; Chu, J. Y.; Nematalla, A.; Wang, X.; Chen, H.; Sistla, A.; Luu, T. C.; Tang, F.; Wei, J.; Tang, C. Discovery of 5-[5-fluoro-2-oxo-1,2-dihydroindol-(3*Z*)-ylidenemethyl]-2,4-dimethyl-1*H*-pyrrole-3-carboxylic acid (2-diethylaminoethyl)amide, a novel tyrosine kinase inhibitor targeting vascular endothelial and platelet-derived growth factor receptor tyrosine kinase. *J. Med. Chem.* **2003**, *46*, 1116−1119.

(14) Lombardo, L. J.; Lee, F. Y.; Chen, P.; Norris, D.; Barrish, J. C.; Behnia, K.; Castaneda, S.; Cornelius, L. A.; Das, J.; Doweyko, A. M.; Fairchild, C.; Hunt, J. T.; Inigo, I.; Johnston, K.; Kamath, A.; Kan, D.; Klei, H.; Marathe, P.; Pang, S.; Peterson, R.; Pitt, S.; Schieven, G. L.; Schmidt, R. J.; Tokarski, J.; Wen, M. L.; Wityak, J.; Borzilleri, R. M. Discovery of *N*-(2-chloro-6-methyl-phenyl)-2-(6-(4-(2-hydroxyethyl)-piperazin-1-yl)-2-methylpyrimidin-4-ylamino)thiazole-5-carboxamide (BMS-354825), a dual Src/Abl kinase inhibitor with potent antitumor activity in preclinical assays. *J. Med. Chem.* **2004**, *47*, 6658−6661.

(15) Davies, S. P.; Reddy, H.; Caivano, M.; Cohen, P. Specificity and mechanism of action of some commonly used protein kinase inhibitors. *Biochem. J.* **2000**, *351*, 95−105.

(16) Bain, J.; McLauchlan, H.; Elliott, M.; Cohen, P. The specificities of protein kinase inhibitors: an update. *Biochem. J.* **2003**, *371*, 199−204.

(17) Blagden, S.; de Bono, J. Drugging cell cycle kinases in cancer therapy. *Curr. Drug Targets* **2005**, *6*, 325−335.

(18) Williamson, D. S.; Parratt, M. J.; Bower, J. F.; Moore, J. D.; Richardson, C. M.; Dokurno, P.; Cansfield, A. D.; Francis, G. L.; Hebdon, R. J.; Howes, R.; Jackson, P. S.; Lockie, A. M.; Murray, J. B.; Nunns, C. L.; Powles, J.; Robertson, A.; Surgenor, A. E.; Torrance, C. J. Structure-guided design of pyrazolo[1,5-*a*]pyrimidines as inhibitors of human cyclin-dependent kinase 2. *Bioorg. Med. Chem. Lett.* **2005**, *15*, 863−867.

(19) Nolen, B.; Taylor, S.; Ghosh, G. Regulation of protein kinases: controlling activity through activation segment conformation. *Mol. Cell* **2004**, *15*, 661−675.

(20) Jacobs, M. D.; Black, J.; Futer, O.; Swenson, L.; Hare, B.; Fleming, M.; Saxena, K. Pim-1 ligand-bound structures reveal the mechanism of serine/threonine kinase inhibition by LY294002. *J. Biol. Chem.* **2005**, *280*, 13728−13734.

(21) Jacobs, M.; Hayakawa, K.; Swenson, L.; Bellon, S.; Fleming, M.; Taslimi, P.; Doran, J. The structure of dimeric ROCK I reveals the mechanism for ligand selectivity. *J. Biol. Chem.* **2006**, *281*, 260−268.

(22) Heron, N. M.; Anderson, M.; Blowers, D. P.; Breed, J.; Eden, J. M.; Green, S.; Hill, G. B.; Johnson, T.; Jung, F. H.; McMiken, H. H.; Mortlock, A. A.; Pannifer, A. D.; Pauptit, R. A.; Pink, J.; Roberts, N. J.; Rowsell, S. SAR and inhibitor complex structure determination of a novel class of potent and specific Aurora kinase inhibitors. *Bioorg. Med. Chem. Lett.* **2006**, *16*, 1320−1323.

(23) Knighton, D. R.; Zheng, J. H.; Ten Eyck, L. F.; Ashford, V. A.; Xuong, N. H.; Taylor, S. S.; Sowadski, J. M. Crystal structure of the catalytic subunit of cyclic adenosine monophosphate-dependent protein kinase. *Science* **1991**, *253*, 407−414.

(24) Brown, N. R.; Noble, M. E.; Endicott, J. A.; Johnson, L. N. The structural basis for specificity of substrate and recruitment peptides for cyclin-dependent kinases. *Nat. Cell Biol.* **1999**, *1*, 438−443.

(25) Huse, M.; Kuriyan, J. The conformational plasticity of protein kinases. *Cell* **2002**, *109*, 275−282.

(26) Liu, Y.; Shah, K.; Yang, F.; Witucki, L.; Shokat, K. M. A molecular gate which controls unnatural ATP analogue recognition by the tyrosine kinase v-Src. *Bioorg. Med. Chem.* **1998**, *6*, 1219−1226.

(27) Shewchuk, L.; Hassell, A.; Wisely, B.; Rocque, W.; Holmes, W.; Veal, J.; Kuyper, L. F. Binding mode of the 4-anilinoquinazoline class of protein kinase inhibitor: X-ray crystallographic studies of 4-anilinoquinazolines bound to cyclin-dependent kinase 2 and p38 kinase. *J. Med. Chem.* **2000**, *43*, 133−138.

(28) Bishop, A. C. A hot spot for protein kinase inhibitor sensitivity. *Chem. Biol.* **2004**, *11*, 587−589.

(29) Cohen, M. S.; Zhang, C.; Shokat, K. M.; Taunton, J. Structural bioinformatics-based design of selective, irreversible kinase inhibitors. *Science* **2005**, *308*, 1318−1321.

(30) Wu, S. Y.; McNae, I.; Kontopidis, G.; McClue, S. J.; McInnes, C.; Stewart, K. J.; Wang, S.; Zheleva, D. I.; Marriage, H.; Lane, D. P.; Taylor, P.; Fischer, P. M.; Walkinshaw, M. D. Discovery of a novel family of CDK inhibitors with the program LIDAEUS: structural basis for ligand-induced disordering of the activation loop. *Structure* **2003**, *11*, 399−410.

(31) Schulze-Gahmen, U.; De Bondt, H. L.; Kim, S. H. High-resolution crystal structures of human cyclin-dependent kinase 2 with and without ATP: bound waters and natural ligand as guides for inhibitor design. *J. Med. Chem.* **1996**, *39*, 4540−4546.

(32) Liao, J. J.-L.; Andrews, R. Targeting protein multiple conformations: a structure-based strategy for kinase drug design. *Curr. Top. Med. Chem.*, in press.

(33) Stamos, J.; Sliwkowski, M. X.; Eigenbrot, C. Structure of the epidermal growth factor receptor kinase domain alone and in complex with a 4-anilinoquinazoline inhibitor. *J. Biol. Chem.* **2002**, *277*, 46265−46272.

(34) Wood, E. R.; Truesdale, A. T.; McDonald, O. B.; Yuan, D.; Hassell, A.; Dickerson, S. H.; Ellis, B.; Pennisi, C.; Horne, E.; Lackey, K.; Alligood, K. J.; Rusnak, D. W.; Gilmer, T. M.; Shewchuk, L. A unique structure for epidermal growth factor receptor bound to GW572016 (Lapatinib): relationships among protein conformation, inhibitor off-rate, and receptor activity in tumor cells. *Cancer Res.* **2004**, *64*, 6652−6659.

(35) Mol, C. D.; Dougan, D. R.; Schneider, T. R.; Skene, R. J.; Kraus, M. L.; Scheibe, D. N.; Snell, G. P.; Zou, H.; Sang, B. C.; Wilson, K. P. Structural basis for the autoinhibition and STI-571 inhibition of c-Kit tyrosine kinase. *J. Biol. Chem.* **2004**, *279*, 31655−31663.

(36) Schindler, T.; Bornmann, W.; Pellicena, P.; Miller, W. T.; Clarkson, B.; Kuriyan, J. Structural mechanism for STI-571 inhibition of Abelson tyrosine kinase. *Science* **2000**, *289*, 1938−1942.

(37) Nagar, B.; Bornmann, W. G.; Pellicena, P.; Schindler, T.; Veach, D. R.; Miller, W. T.; Clarkson, B.; Kuriyan, J. Crystal structures of the kinase domain of c-Abl in complex with the small molecule inhibitors PD173955 and imatinib (Sti-571). *Cancer Res.* **2002**, *62*, 4236−4243.

(38) Wan, P. T. C.; Garnett, M. J.; Roe, S. M.; Lee, S.; Niculescu-Duvaz, D.; Good, V. M.; Jones, C. M.; Marshall, C. J.; Springer, C. J.; Barford, D.; Marais, R. Cancer Genome Project. Mechanism of activation of the Raf-Erk signaling pathway by oncogenic mutations of B-Raf. *Cell* **2004**, *116*, 855−867.

(39) Pargellis, C.; Tong, L.; Churchill, L.; Cirillo, P. F.; Gilmore, T.; Graham, A. G.; Grob, P. M.; Hickey, E. R.; Moss, N.; Pav, S.; Regan, J. Inhibition of p38 Map kinase by utilizing a novel allosteric binding site. *Nat. Struct. Biol.* **2002**, *9*, 268−272.

(40) Jung, F. H.; Pasquet, G.; Lambert-van der Brempt, C.; Lohmann, J. J.; Warin, N.; Renaud, F.; Germain, H.; De Savi, C.; Roberts, N.; Johnson, T.; Dousson, C.; Hill, G. B.; Mortlock, A. A.; Heron, N.; Wilkinson, R. W.; Wedge, S. R.; Heaton, S. P.; Odedra, R.; Keen, N. J.; Green, S.; Brown, E.; Thompson, K.; Brightwell, S. Discovery of novel and potent thiazoloquinazolines as selective Aurora A and B kinase inhibitors. *J. Med. Chem.* **2006**, *49*, 955−970.

(41) Fabbro, D.; Ruetz, S.; Buchdunger, E.; Cowan-Jacob, S. W.; Fendrich, G.; Liebetanz, J.; Mestan, J.; O'Reilly, T.; Traxler, P.; Chaudhuri, B.; Fretz, H.; Zimmermann, J.; Meyer, T.; Caravatti, G.; Furet, P.; Manley, P. W. Protein kinases as targets for anticancer agents: from inhibitors to useful drugs. *Pharmacol. Ther.* **2002**, *93*, 79−98.

(42) Cherry, M.; Williams, D. H. Recent kinase and kinase inhibitor X-ray structures: Mechanisms of inhibition and selectivity insights. *Curr. Med. Chem.* **2004**, *11*, 663−673.

(43) Yang, J.; Cron, P.; Good, V. M.; Thompson, V.; Hemmings, B. A.; Barford, D. Crystal structure of an activated Akt/protein kinase B ternary complex with GSK3-peptide and AMP-PNP. *Nat. Struct. Biol.* **2002**, *9*, 940−944.

(44) Zheng, J.; Trafny, E. A.; Knighton, D. R.; Xuong, N. H.; Taylor, S. S.; Teneyck, L. F.; Sowadski, J. M. 2.2 Å refined crystal structure of the catalytic subunit of cAMP-dependent protein kinase complexed with MnATP and a peptide inhibitor. *Acta Crystallogr., Sect. D: Biol. Crystallogr.* **1993**, *49*, 362−365.

(45) Battistutta, R.; Sarno, S.; De Moliner, E.; Papinutto, E.; Zanotti, G.; Pinna, L. A. The replacement of ATP by the competitive inhibitor emodin induces conformational modifications in the catalytic site of protein kinase CK2. *J. Biol. Chem.* **2000**, *275*, 29618−29622.

(46) De Moliner, E.; Brown, N. R.; Johnson, L. N. Alternative binding modes of an inhibitor to two different kinases. *Eur. J. Biochem.* **2003**, *270*, 3174−3181.

(47) Pinna, L. A. The raison d'etre of constitutively active protein kinases: The lesson of CK2. *Acc. Chem. Res.* **2003**, *36*, 378−384.

(48) Battistutta, R.; Mazzorana, M.; Sarno, S.; Kazimierczuk, Z.; Zanotti, G.; Pinna, L. A. Inspecting the structure−activity relationship of protein kinase CK2 inhibitors derived from tetrabromo-benzimidazole. *Chem. Biol.* **2005**, *12*, 1211−1219.

(49) Yde, C. W.; Ermakova, I.; Issinger, O. G.; Niefind, K. Inclining the purine base binding plane in protein kinase CK2 by exchanging the flanking side-chains generates a preference for ATP as a cosubstrate. *J. Mol. Biol.* **2005**, *347*, 399−414.

(50) Jautelat, R.; Brumby, T.; Schäfer, M.; Briem, H.; Eisenbrand, G.; Schwahn, S.; Krüger, M.; Lücking, U.; Prien, O.; Siemeister, G. From the insoluble dye indirubin towards highly active, soluble CDK2-inhibitors. *ChemBioChem* **2005**, *6*, 531−540.

(51) Kontopidis, G.; McInnes, C.; Pandalaneni, S. R.; McNae, I.; Gibson, D.; Mezna, M.; Thomas, M.; Wood, G.; Wang, S.; Walkinshaw, M. D.; Fischer, P. M. Differential binding of inhibitors to active and inactive CDK2 provides insights for drug design. *Chem. Biol.* **2006**, *13*, 201−211.
(52) Wang, Z.; Canagarajah, B. J.; Boehm, J. C.; Kassisa, S.; Cobb, M. H.; Young, P. R.; Abdel-Meguid, S.; Adams, J. L.; Goldsmith, E. J. Structural basis of inhibitor selectivity in MAP kinases. *Structure* **1998**, *6*, 1117−1128.
(53) Schindler, T.; Sicheri, F.; Pico, A.; Gazit, A.; Levitzki, A.; Kuriyan, J. Crystal structure of Hck in complex with a Src family-selective tyrosine kinase inhibitor. *Mol. Cell* **1999**, *3*, 639−648.
(54) Carter, M. C.; Cockerill, G. S.; Guntrip, S. B.; Lackey, K. E.; Smith, K. J. Bicyclic heteroaromatic compounds (quinazolinamines and analogs) useful as protein tyrosine kinase inhibitors. PCT Int. Appl. WO9935146, 1999; Glaxo Wellcome.
(55) Hubbard, S. R.; Wei, L.; Ellis, L.; Hendrickson, W. A. Crystal structure of the tyrosine kinase domain of the human insulin receptor. *Nature* **1994**, *372*, 746−754.
(56) Miyazaki, Y.; Matsunaga, S.; Tang, J.; Maeda, Y.; Nakano, M.; Philippe, R. J.; Shibahara, M.; Liu, W.; Sato, H.; Wang, L.; Nolte, R. T. Novel 4-amino-furo[2,3-*d*]pyrimidines as Tie-2 and VEGFR2 dual inhibitors. *Bioorg. Med. Chem. Lett.* **2005**, *15*, 2203−2207.
(57) Harris, P. A.; Cheung, M.; Hunter, R. N., 3rd; Brown, M. L.; Veal, J. M.; Nolte, R. T.; Wang, L.; Liu, W.; Crosby, R. M.; Johnson, J. H.; Epperly, A. H.; Kumar, R.; Luttrell, D. K.; Stafford, J. A. Discovery and evaluation of 2-anilino-5-aryloxazoles as a novel class of VEGFR2 kinase inhibitors. *J. Med. Chem.* **2005**, *48*, 1610−1619.
(58) Griffith, J.; Black, J.; Faerman, C.; Swenson, L.; Wynn, M.; Lu, F.; Lippke, J.; Saxena, K. The structural basis for autoinhibition of FLT3 by the juxtamembrane domain. *Mol. Cell* **2004**, *13*, 169−178.
(59) Nagar, B.; Hantschel, O.; Young, M. A.; Scheffzek, K.; Veach, D.; Bornmann, W.; Clarkson, B.; Superti-Furga, G.; Kuriyan, J. Structural basis for the autoinhibition of c-Abl tyrosine kinase. *Cell* **2003**, *112*, 859−871.
(60) Wisniewski, D.; Lambek, C. L.; Liu, C.; Strife, A.; Veach, D. R.; Nagar, B.; Young, M. A.; Schindler, T.; Bornmann, W. G.; Bertino, J. R.; Kuriyan, J.; Clarkson, B. Characterization of potent inhibitors of the Bcr-Abl and the c-kit receptor tyrosine kinases. *Cancer Res.* **2002**, *62*, 4244−4255.
(61) Mol, C. D.; Lim, K. B.; Sridhar, V.; Zou, H.; Chien, E. Y.; Sang, B. C.; Nowakowski, J.; Kassel, D. B.; Cronin, C. N.; McRee, D. E. Structure of a c-Kit product complex reveals the basis for kinase transactivation. *J. Biol. Chem.* **2003**, *278*, 31461−31464.
(62) Nowakowski, J.; Cronin, C. N.; McRee, D. E.; Knuth, M. W.; Nelson, C. G.; Pavletich, N. P.; Rogers, J.; Sang, B. C.; Scheibe, D. N.; Swanson, R. V.; Thompson, D. A. Structures of the cancer-related Aurora-A, FAK, and EphA2 protein kinases from nanovolume crystallography. *Structure* **2002**, *10*, 1659−1667.
(63) Bayliss, R.; Sardon, T.; Vernos, I.; Conti, E. Structural basis of Aurora-A activation by Tpx2 at the mitotic spindle. *Mol. Cell* **2003**, *12*, 851−862.
(64) Hamby, J. M.; Connolly, C. J.; Schroeder, M. C.; Winters, R. T.; Showalter, H. D.; Panek, R. L.; Major, T. C.; Olsewski, B.; Ryan, M. J.; Dahring, T.; Lu, G. H.; Keiser, J.; Amar, A.; Shen, C.; Kraker, A. J.; Slintak, V.; Nelson, J. M.; Fry, D. W.; Bradford, L.; Hallak, H.; Doherty, A. M. Structure−activity relationships for a novel series of pyrido[2,3-*d*]pyrimidine tyrosine kinase inhibitors. *J. Med. Chem.* **1997**, *40*, 2296−2303.
(65) Gohlke, H.; Klebe, G. Approaches to the description and prediction of the binding affinity of small-molecule ligands to macromolecular receptors. *Angew. Chem., Int. Ed.* **2002**, *41*, 2644−2676.
(66) Auffinger, P.; Hays, F. A.; Westhof, E.; Ho, P. S. Halogen bonds in biological molecules. *Proc. Natl. Acad. Sci. U.S.A.* **2004**, *101*, 16789−16794.
(67) Ajay; Murcko, M. A. Computational methods to predict binding free energy in ligand−receptor complexes. *J. Med. Chem.* **1995**, *38*, 4953−4967.
(68) Barnett, S. F.; Bilodeau, M. T.; Lindsley, C. W. The Akt/PKB family of protein kinases: A review of small molecule inhibitors and progress towards target validation. *Curr. Top. Med. Chem.* **2005**, *5*, 109−125.
(69) Mortlock, A.; Keen, N. J.; Jung, F. H.; Heron, N. M.; Foote, K. M.; Wilkinson, R.; Green, S. Progress in the development of selective inhibitors of Aurora kinases. *Curr. Top. Med. Chem.* **2005**, *5*, 199−213.
(70) Wallace, E. M.; Lyssikatos, J. P.; Yeh, T.; Winkler, J. D.; Koch, K. Progress towards therapeutic small molecule MEK inhibitors for use in cancer therapy. *Curr. Top. Med. Chem.* **2005**, *5*, 215−229.
(71) Hiroshi, H.; Nobuhiko, K.; Yoshikazu, I. Recent advances in the development of selective small molecule inhibitors for cyclin-dependent kinases. *Curr. Top. Med. Chem.* **2005**, *5*, 167−179.
(72) Benson, C.; Kaye, S.; Workman, P.; Garrett, M.; Walton, M.; de Bono, J. Clinical anticancer drug development: targeting the cyclin-dependent kinases. *Br. J. Cancer* **2005**, *92*, 7−12.
(73) Senderowicz, A. M. Small-molecule cyclin-dependent kinase modulators. *Oncogene* **2003**, *22*, 6609−6620.
(74) Sielecki, T. M.; Boylan, J. F.; Benfield, P. A.; Trainor, G. L. Cyclin-dependent kinase inhibitors: useful targets in cell cycle regulation. *J. Med. Chem.* **2000**, *43*, 1−18.
(75) Vesely, J.; Havlicek, L.; Strnad, M.; Blow, J. J.; Donella-Deana, A.; Pinna, L.; Letham, D. S.; Kato, J.; Detivaud, L.; Leclerc, S.; Meijer, L. Inhibition of cyclin-dependent kinases by purine analogues. *Eur. J. Biochem.* **1994**, *224*, 771−786.
(76) De Azevedo, W. F.; Leclerc, S.; Meijer, L.; Havlicek, L.; Strnad, M.; Kim, S. H. Inhibition of cyclin-dependent kinases by purine analogues: crystal structure of human cdk2 complexed with roscovitine. *Eur. J. Biochem.* **1997**, *243*, 518−526.
(77) Dreyer, M. K.; Borcherding, D. R.; Dumont, J. A.; Peet, N. P.; Tsay, J. T.; Wright, P. S.; Bitonti, A. J.; Shen, J.; Kim, S. H. Crystal structure of human cyclin-dependent kinase 2 in complex with the adenine-derived inhibitor H717. *J. Med. Chem.* **2001**, *44*, 524−530.
(78) Haesslein, J. L.; Jullian, N. Recent advances in cyclin-dependent kinase inhibition. Purine-based derivatives as anti-cancer agents. Roles and perspectives for the future. *Curr. Top. Med. Chem.* **2002**, *2*, 1037−1050.
(79) Meijer, L.; Raymond, E. Roscovitine and other purines as kinase inhibitors. From starfish oocytes to clinical trials. *Acc. Chem. Res.* **2003**, *36*, 417−425.
(80) Gray, N. S.; Wodicka, L.; Thunnissen, A. M.; Norman, T. C.; Kwon, S.; Espinoza, F. H.; Morgan, D. O.; Barnes, G.; LeClerc, S.; Meijer, L.; Kim, S. H.; Lockhart, D. J.; Schultz, P. G. Exploiting chemical libraries, structure, and genomics in the search for kinase inhibitors. *Science* **1998**, *281*, 533−538.
(81) Chang, Y. T.; Gray, N. S.; Rosania, G. R.; Sutherlin, D. P.; Kwon, S.; Norman, T. C.; Sarohia, R.; Leost, M.; Meijer, L.; Schultz, P. G. Synthesis and application of functionally diverse 2,6,9-trisubstituted purine libraries as CDK inhibitors. *Chem. Biol.* **1999**, *6*, 361−375.
(82) De Bondt, H. L.; Rosenblatt, J.; Jancarik, J.; Jones, H. D.; Morgan, D. O.; Kim, S. H. Crystal structure of cyclin-dependent kinase 2. *Nature* **1993**, *363*, 595−602.
(83) Schulze-Gahmen, U.; Brandsen, J.; Jones, H. D.; Morgan, D. O.; Meijer, L.; Vesely, J.; Kim, S. H. Multiple modes of ligand recognition: crystal structures of cyclin-dependent protein kinase 2 in complex with ATP and two inhibitors, olomoucine and isopentenyladenine. *Proteins* **1995**, *22*, 378−391.
(84) Krystof, V.; McNae, I. W.; Walkinshaw, M. D.; Fischer, P. M.; Muller, P.; Vojtesek, B.; Orsag, M.; Havlicek, L.; Strnad, M. Antiproliferative activity of olomoucine II, a novel 2,6,9-trisubstituted purine cyclin-dependent kinase inhibitor. *Cell. Mol. Life Sci.* **2005**, *62*, 1763−1771.
(85) Misra, R. N.; Xiao, H. Y.; Kim, K. S.; Lu, S.; Han, W. C.; Barbosa, S. A.; Hunt, J. T.; Rawlins, D. B.; Shan, W.; Ahmed, S. Z.; Qian, L.; Chen, B. C.; Zhao, R.; Bednarz, M. S.; Kellar, K. A.; Mulheron, J. G.; Batorsky, R.; Roongta, U.; Kamath, A.; Marathe, P.; Ranadive, S. A.; Sack, J. S.; Tokarski, J. S.; Pavletich, N. P.; Lee, F. Y.; Webster, K. R.; Kimball, S. D. *N*-(Cycloalkylamino)acyl-2-aminothiazole inhibitors of cyclin-dependent kinase 2. *N*-[5-[[[5-(1,1-Dimethylethyl)-2-oxazolyl]methyl]thio]-2-thiazolyl]-4-piperidinecarboxamide (BMS-387032), a highly efficacious and selective antitumor agent. *J. Med. Chem.* **2004**, *47*, 1719−1728.
(86) Fancelli, D.; Berta, D.; Bindi, S.; Cameron, A.; Cappella, P.; Carpinelli, P.; Catana, C.; Forte, B.; Giordano, P.; Giorgini, M. L.; Mantegani, S.; Marsiglio, A.; Meroni, M.; Moll, J.; Pittala, V.; Roletto, F.; Severino, D.; Soncini, C.; Storici, P.; Tonani, R.; Varasi, M.; Vulpetti, A.; Vianello, P. Potent and selective Aurora inhibitors identified by the expansion of a novel scaffold for protein kinase inhibition. *J. Med. Chem.* **2005**, *48*, 3080−3084.
(87) Pevarello, P.; Fancelli, D.; Vulpetti, A.; Amici, R.; Villa, M.; Pittala, V.; Vianello, P.; Cameron, A.; Ciomei, M.; Mercurio, C.; Bischoff, J. R.; Roletto, F.; Varasi, M.; Brasca, M. G. 3-Amino-1,4,5,6-tetrahydropyrrolo[3,4-C]pyrazoles: a new class of Cdk2 inhibitors. *Bioorg. Med. Chem. Lett.* **2006**, *16*, 1084−1090.
(88) Mohammadi, M.; McMahon, G.; Sun, L.; Tang, C.; Hirth, P.; Yeh, B. K.; Hubbard, S. R.; Schlessinger, J. Structures of the tyrosine kinase domain of fibroblast growth factor receptor in complex with inhibitors. *Science* **1997**, *276*, 955−960.
(89) Laird, A. D.; Vajkoczy, P.; Shawver, L. K.; Thurnher, A.; Liang, C.; Mohammadi, M.; Schlessinger, J.; Ullrich, A.; Hubbard, S. R.; Blake, R. A.; Fong, T. A.; Strawn, L. M.; Sun, L.; Tang, C.; Hawtin, R.; Tang, F.; Shenoy, N.; Hirth, K. P.; McMahon, G.; Cherrington, J. M. SU6668 is a potent antiangiogenic and antitumor agent that induces regression of established tumors. *Cancer Res.* **2000**, *60*, 4152−4160.

(90) Abrams, T. J.; Lee, L. B.; Murray, L. J.; Pryer, N. K.; Cherrington, J. M. SU11248 inhibits KIT and platelet-derived growth factor receptor β in preclinical models of human small cell lung cancer. *Mol. Cancer Ther.* **2003**, *2*, 471−478.
(91) Mendel, D. B.; Laird, A. D.; Xin, X.; Louie, S. G.; Christensen, J. G.; Li, G.; Schreck, R. E.; Abrams, T. J.; Ngai, T. J.; Lee, L. B.; Murray, L. J.; Carver, J.; Chan, E.; Moss, K. G.; Haznedar, J. O.; Sukbuntherng, J.; Blake, R. A.; Sun, L.; Tang, C.; Miller, T.; Shirazian, S.; McMahon, G.; Cherrington, J. M. In vivo antitumor activity of SU11248, a novel tyrosine kinase inhibitor targeting vascular endothelial growth factor and platelet-derived growth factor receptors: Determination of a pharmacokinetic/pharmacodynamic relationship. *Clin. Cancer Res.* **2003**, *9*, 327−337.
(92) Motzer, R.; Hoosen, S.; Bello, C. L.; Christensen, J. G. Sunitinib malate for the treatment of solid tumours: a review of current clinical data. *Expert Opin. Invest. Drugs* **2006**, *15*, 553−561.
(93) Eskens, F. A. Angiogenesis inhibitors in clinical development; where are we now and where are we going? *Br. J. Cancer* **2004**, *90*, 1−7.
(94) Faivre, S.; Delbaldo, C.; Vera, K.; Robert, C.; Lozahic, S.; Lassau, N.; Bello, C.; Deprimo, S.; Brega, N.; Massimini, G.; Armand, J. P.; Scigalla, P.; Raymond, E. Safety, pharmacokinetic, and antitumor activity of SU11248, a novel oral multitarget tyrosine kinase inhibitor, in patients with cancer. *J. Clin. Oncol.* **2006**, *24*, 25−35.
(95) Uehata, M.; Ishizaki, T.; Satoh, H.; Ono, T.; Kawahara, T.; Morishita, T.; Tamakawa, H.; Yamagami, K.; Inui, J.; Maekawa, M.; Narumiya, S. Calcium sensitization of smooth muscle mediated by a Rho-associated protein kinase in hypertension. *Nature* **1997**, *389*, 990−994.
(96) Shimokawa, H.; Seto, M.; Katsumata, N.; Amano, M.; Kozai, T.; Yamawaki, T.; Kuwata, K.; Kandabashi, T.; Egashira, K.; Ikegaki, I.; Asano, T.; Kaibuchi, K.; Takeshita, A. Rho-kinase-mediated pathway induces enhanced myosin light chain phosphorylations in a swine model of coronary artery spasm. *Cardiovasc. Res.* **1999**, *43*, 1029−1039.
(97) Ono-Saito, N.; Niki, I.; Hidaka, H. H-series protein kinase inhibitors and potential clinical applications. *Pharmacol. Ther.* **1999**, *82*, 123−131.
(98) Mueller, B. K.; Mack, H.; Teusch, N. Rho kinase, a promising drug target for neurological disorders. *Nat. Rev. Drug Discovery* **2005**, *4*, 387−398.
(99) Rusnak, D. W.; Lackey, K.; Affleck, K.; Wood, E. R.; Alligood, K. J.; Rhodes, N.; Keith, B. R.; Murray, D. M.; Knight, W. B.; Mullin, R. J.; Gilmer, T. M. The effects of the novel, reversible epidermal growth factor receptor/ErbB-2 tyrosine kinase inhibitor, GW572016, on the growth of human normal and tumor-derived cell lines in vitro and in vivo. *Mol. Cancer Ther.* **2001**, *1*, 85−94.
(100) Harrington, E. A.; Bebbington, D.; Moore, J.; Rasmussen, R. K.; Ajose-Adeogun, A. O.; Nakayama, T.; Graham, J. A.; Demur, C.; Hercend, T.; Diu-Hercend, A.; Su, M.; Golec, J. M.; Miller, K. M. VX-680, a potent and selective small-molecule inhibitor of the Aurora kinases, suppresses tumor growth in vivo. *Nat. Med.* **2004**, *10*, 262−267.
(101) Carter, T. A.; Wodicka, L. M.; Shah, N. P.; Velasco, A. M.; Fabian, M. A.; Treiber, D. K.; Milanov, Z. V.; Atteridge, C. E.; Biggs, W. H., 3rd; Edeen, P. T.; Floyd, M.; Ford, J. M.; Grotzfeld, R. M.; Herrgard, S.; Insko, D. E.; Mehta, S. A.; Patel, H. K.; Pao, W.; Sawyers, C. L.; Varmus, H.; Zarrinkar, P. P.; Lockhart, D. J. Inhibition of drug-resistant mutants of ABL, KIT, and EGF receptor kinases. *Proc. Natl. Acad. Sci. U.S.A.* **2005**, *102*, 11011−11016.
(102) Young, M. A.; Shah, N. P.; Chao, L. H.; Seeliger, M.; Milanov, Z. V.; Biggs, W. H., 3rd; Treiber, D. K.; Patel, H. K.; Zarrinkar, P. P.; Lockhart, D. J.; Sawyers, C. L.; Kuriyan, J. Structure of the kinase domain of an imatinib-resistant Abl mutant in complex with the Aurora kinase inhibitor VX-680. *Cancer Res.* **2006**, *66*, 1007−1014.
(103) Martinelli, G.; Soverini, S.; Rosti, G.; Baccarani, M. Dual tyrosine kinase inhibitors in chronic myeloid leukemia. *Leukemia* **2005**, *19*, 1872−1879.
(104) O'Hare, T.; Pollock, R.; Stoffregen, E. P.; Keats, J. A.; Abdullah, O. M.; Moseson, E. M.; Rivera, V. M.; Tang, H.; Metcalf, C. A., 3rd; Bohacek, R. S.; Wang, Y.; Sundaramoorthi, R.; Shakespeare, W. C.; Dalgarno, D.; Clackson, T.; Sawyer, T. K.; Deininger, M. W.; Druker, B. J. Inhibition of wild-type and mutant Bcr-Abl by AP23464, a potent ATP-based oncogenic protein kinase inhibitor: implications for CML. *Blood* **2004**, *104*, 2532−2539.
(105) Dalgarno, D.; Stehle, T.; Narula, S.; Schelling, P.; van Schravendijk, M. R.; Adams, S.; Andrade, L.; Keats, J.; Ram, M.; Jin, L.; Grossman, T.; MacNeil, I.; Metcalf, C., 3rd; Shakespeare, W.; Wang, Y.; Keenan, T.; Sundaramoorthi, R.; Bohacek, R.; Weigele, M.; Sawyer, T. Structural basis of Src tyrosine kinase inhibition with a new class of potent and selective trisubstituted purine-based compounds. *Chem. Biol. Drug Des.* **2006**, *67*, 46−57.
(106) Sicheri, F.; Moarefi, I.; Kuriyan, J. Crystal structure of the Src family tyrosine kinase Hck. *Nature* **1997**, *385*, 602−609.
(107) Missbach, M.; Jeschke, M.; Feyen, J.; Muller, K.; Glatt, M.; Green, J.; Susa, M. A novel inhibitor of the tyrosine kinase Src suppresses phosphorylation of its major cellular substrates and reduces bone resorption in vitro and in rodent models in vivo. *Bone* **1999**, *24*, 437−449.
(108) Breitenlechner, C. B.; Kairies, N. A.; Honold, K.; Scheiblich, S.; Koll, H.; Greiter, E.; Koch, S.; Schafer, W.; Huber, R.; Engh, R. A. Crystal structures of active Src kinase domain complexes. *J. Mol. Biol.* **2005**, *353*, 222−231.
(109) Boschelli, D. H.; Wu, Z.; Klutchko, S. R.; Showalter, H. D.; Hamby, J. M.; Lu, G. H.; Major, T. C.; Dahring, T. K.; Batley, B.; Panek, R. L.; Keiser, J.; Hartl, B. G.; Kraker, A. J.; Klohs, W. D.; Roberts, B. J.; Patmore, S.; Elliott, W. L.; Steinkampf, R.; Bradford, L. A.; Hallak, H.; Doherty, A. M. Synthesis and tyrosine kinase inhibitory activity of a series of 2-amino-8*H*-pyrido[2,3-*d*]pyrimidines: identification of potent, selective platelet-derived growth factor receptor tyrosine kinase inhibitors. *J. Med. Chem.* **1998**, *41*, 4365−4377.
(110) Ohren, J. F.; Chen, H.; Pavlovsky, A.; Whitehead, C.; Zhang, E.; Kuffa, P.; Yan, C.; McConnell, P.; Spessard, C.; Banotai, C.; Mueller, W. T.; Delaney, A.; Omer, C.; Sebolt-Leopold, J.; Dudley, D. T.; Leung, I. K.; Flamme, C.; Warmus, J.; Kaufman, M.; Barrett, S.; Tecle, H.; Hasemann, C. A. Structures of human MAP kinase kinase 1 (MEK1) and MEK2 describe novel noncompetitive kinase inhibition. *Nat. Struct. Mol. Biol.* **2004**, *11*, 1192−1197.
(111) Druker, B. J.; Lydon, N. B. Lessons learned from the development of an Abl tyrosine kinase inhibitor for chronic myelogenous leukemia. *J. Clin. Invest.* **2000**, *105*, 3−7.
(112) Ahmad, T.; Eisen, T. Kinase inhibition with BAY 43-9006 in renal cell carcinoma. *Clin. Cancer Res.* **2004**, *10*, 6388s−6392s.
(113) Doble, B. W.; Woodgett, J. R. GSK-3: tricks of the trade for a multitasking kinase. *J. Cell Sci.* **2003**, *116*, 1175−1186.
(114) Breitenlechner, C.; Gassel, M.; Hidaka, H.; Kinzel, V.; Huber, R.; Engh, R. A.; Bossemeyer, D. Protein kinase A in complex with Rho-kinase-inhibitors Y-27632, fasudil and H-1152P: structural basis of selectivity. *Structure* **2003**, *11*, 1595−1607.
(115) Richardson, C. M.; Williamson, D. S.; Parratt, M. J.; Borgognoni, J.; Cansfield, A. D.; Dokurno, P.; Francis, G. L.; Howes, R.; Moore, J. D.; Murray, J. B.; Robertson, A.; Surgenor, A. E.; Torrance, C. J. Triazolo[1,5-A]pyrimidines as novel Cdk2 inhibitors: protein structure-guided design and SAR. *Bioorg. Med. Chem. Lett.* **2006**, *16*, 1353−1357.
(116) Knight, Z. A.; Shokat, K. M. Features of selective kinase inhibitors. *Chem. Biol.* **2005**, *12*, 621−637.
(117) Fitzgerald, C. E.; Patel, S. B.; Becker, J. W.; Cameron, P. M.; Zaller, D.; Pikounis, V. B.; O'Keefe, S. J.; Scapin, G. Structural basis for p38α MAP kinase quinazolinone and pyridol-pyrimidine inhibitor specificity. *Nat. Struct. Biol.* **2003**, *10*, 764−769.
(118) Bischoff, J. R.; Anderson, L.; Zhu, Y.; Mossie, K.; Ng, L.; Souza, B.; Schryver, B.; Flanagan, P.; Clairvoyant, F.; Ginther, C.; Chan, C. S.; Novotny, M.; Slamon, D. J.; Plowman, G. D. A homologue of Drosophila aurora kinase is oncogenic and amplified in human colorectal cancers. *EMBO J.* **1998**, *17*, 3052−3065.
(119) Hardy, L. W.; Peet, N. P. The multiple orthogonal tools approach to define molecular causation in the validation of druggable targets. *Drug Discovery Today* **2004**, *9*, 117−126.
(120) Dancey, J.; Sausville, E. A. Issues and progress with protein kinase inhibitors for cancer treatment. *Nat. Rev. Drug Discovery* **2003**, *2*, 296−313.
(121) Blume-Jensen, P.; Hunter, T. Oncogenic kinase signalling. *Nature* **2001**, *411*, 355−365.
(122) Lynch, T. J.; Bell, D. W.; Sordella, R.; Gurubhagavatula, S.; Okimoto, R. A.; Brannigan, B. W.; Harris, P. L.; Haserlat, S. M.; Supko, J. G.; Haluska, F. G.; Louis, D. N.; Christiani, D. C.; Settleman, J.; Haber, D. A. Activating mutations in the epidermal growth factor receptor underlying responsiveness of non-small cell lung cancer to gefitinib. *N. Engl. J. Med.* **2004**, *350*, 2129−2139.
(123) Cohen, M. H.; Williams, G. A.; Sridhara, R.; Chen, G.; McGuinn, W. D.; Morse, D., Jr.; Abraham, S.; Rahman, A.; Liang, C.; Lostritto, R.; Baird, A.; Pazdur, R. United States Food and Drug Administration drug approval summary gefitinib (ZD1839; Iressa) tablets. *Clin. Cancer Res.* **2004**, *10*, 1212−1218.
(124) Vieth, M.; Sutherland, J. J.; Robertson, D. H.; Campbell, R. M. Kinomics: characterizing the therapeutically validated kinase space. *Drug Discovery Today* **2005**, *10*, 839−846.
(125) van de Waterbeemd, H.; Smith, D. A.; Beaumont, K.; Walker, D. A. Property-based design: optimization of drug absorption and pharmacokinetics. *J. Med. Chem.* **2001**, *44*, 1313−1333.

(126) Lipinski, C. A.; Lombardo, F.; Dominy, B. W.; Feeney, P. J. Experimental and computational approaches to estimate solubility and permeability in drug discovery and development. *Adv. Drug Delivery Rev.* **2001**, *46*, 3−26.
(127) Lipinski, C. A. Drug-like properties and the causes of poor solubility and poor permeability. *J. Pharmacol. Toxicol. Methods* **2000**, *44*, 235−249.
(128) Seelig, A. A general pattern for substrate recognition by P-glycoprotein. *Eur. J. Biochem.* **1998**, *251*, 252−261.
(129) Martin, Y. C. A bioavailability score. *J. Med. Chem.* **2005**, *48*, 3164−3170.
(130) Clark, R. D.; Wolohan, P. R. Molecular design and bioavailability. *Curr. Top. Med. Chem.* **2003**, *3*, 1269−1288.
(131) Kuntz, I. D.; Blaney, J. M.; Oatley, S. J.; Langridge, R.; Ferrin, T. E. A geometric approach to macromolecule−ligand interactions. *J. Mol. Biol.* **1982**, *161*, 269−288.
(132) Warren, G. L.; Andrews, C. W.; Capelli, A.-M.; Clarke, B.; LaLonde, J.; Lambert, M. H.; Lindvall, M.; Nevins, N.; Semus, S. F.; Senger, S.; Tedesco, G.; Wall, I. D.; Woolven, J. M.; Peishoff, C. E.; Head, M. S. A critical assessment of docking programs and scoring functions. *J. Med. Chem.* **2006**, *49*, 5912−5931.
(133) Kitchen, D. B.; Decornez, H.; Furr, J. R.; Bajorath, J. Docking and scoring in virtual screening for drug discovery: methods and applications. *Nat. Rev. Drug Discovery* **2004**, *3*, 935−949.

JM0608107